

Clinical use of intracoronary imaging. Part 2: acute coronary syndromes, ambiguous coronary angiography findings, and guiding interventional decision-making: an expert consensus document of the European Association of Percutaneous Cardiovascular Interventions



Thomas W. Johnson¹, Lorenz Räber², Carlo di Mario³, Christos Bourantas⁴, Haibo Jia⁵, Alessio Mattesini⁴, Nieves Gonzalo⁶, Jose M. de la Torre Hernandez⁷, Francesco Prati⁸, Konstantinos Koskinas², Michael Joner⁹, Maria D. Radu¹⁰, David Erlinge¹¹, Evelyn Regar¹², Vijay Kunadian¹³, Akiko Maehara¹⁴, Robert A. Byrne⁹, Davide Capodanno¹⁵, Takashi Akasaka¹⁶, William Wijns¹⁷, Gary S. Mintz¹⁴, Giulio Guagliumi^{18*}

The authors' affiliations can be found in the Appendix paragraph.

Endorsed by the Chinese Society of Cardiology, the Hong Kong Society of Transcatheter Endocardiovascular Therapeutics (HKSTENT) and the Cardiac Society of Australia and New Zealand

This paper also includes supplementary data published online at: https://eurointervention.pconline.com/doi/10.4244/EIJY19M06_02

KEYWORDS

- percutaneous coronary intervention
- intravascular imaging
- intravascular ultrasound
- optical coherence tomography
- acute coronary syndrome

This consensus document is the second of two reports summarizing the views of an expert panel organized by the European Association of Percutaneous Cardiovascular Interventions (EAPCI) on the clinical use of intracoronary imaging including intravascular ultrasound (IVUS), optical coherence tomography (OCT), and near infrared spectroscopy (NIRS)-IVUS. Beyond guidance of stent selection and optimization of deployment, invasive imaging facilitates angiographic interpretation and may guide treatment in acute coronary syndrome. Intravascular imaging can provide additional important diagnostic information when confronted with angiographically ambiguous lesions and allows assessment of plaque morphology enabling identification of vulnerability characteristics. This second document focuses on useful imaging features to identify culprit and vulnerable coronary plaque, which offers the interventional cardiologist guidance on when to adopt an intracoronary imaging-guided approach to the treatment of coronary artery disease and provides an appraisal of intravascular imaging-derived metrics to define the haemodynamic significance of coronary lesions.

* Corresponding author. Tel: +39 035 2673452; Fax: +39 035 2674964. E-mail: guagliumig@gmail.com.

The article has been co-published with permission in the *European Heart Journal* and *EuroIntervention*. All rights reserved.

© The Author(s) 2019. The articles are identical except for minor stylistic and spelling differences in keeping with each journal's style. Either citation can be used when citing this article.

Preamble

This consensus document, a summary of the views of an expert panel organized by the European Association of Percutaneous Cardiovascular Interventions (EAPCI), appraises current evidence on clinical indications for intracoronary imaging and provides guidance to the interventional community regarding recommended use, strengths, and potential limitations of intravascular ultrasound (IVUS), optical coherence tomography (OCT), and near infrared spectroscopy (NIRS)-IVUS based on existing evidence and the best current practice. The selection of the expert group, the organization of manuscript preparation and consensus development were detailed in Part 1.¹

Introduction

The role of intracoronary imaging to enhance the outcome of percutaneous coronary intervention (PCI), particularly through patient selection and criteria for guiding stent optimization was outlined in Part 1.¹ Our consensus opinion has been strengthened by recent European guidelines enhancing the recommendation for use of OCT for stent optimization to Class IIa.² Furthermore, a trial of IVUS- vs. angio-guided PCI has confirmed a reduction in target vessel failure at 12 months through IVUS-guided optimization³; and updated meta-analyses now indicate a mortality advantage.⁴ Extending the role of intracoronary imaging, requires a shift in focus from the PCI to pre-PCI assessment of the coronary vasculature. Part 2 will focus on the use of intravascular imaging in patients presenting with acute coronary syndrome (ACS), and its role in defining the composition of atherosclerotic plaque, particularly detection of culprit lesions and markers of vulnerability. Additionally, we will emphasize the role of intravascular imaging when angiographic assessment is ambiguous or inconclusive, and its potential for assessing stenosis haemodynamic significance. We believe these extended benefits of intracoronary imaging will provide considerable value to the interventional community and their patients; however, we acknowledge that large scale, robust data is lacking in many of these fields. This strengthens the need for our consensus document to provide clinicians with guidance on the application of intracoronary imaging modalities.

Editorial, see page 392

Acute coronary syndromes

The greatest impact of PCI has been observed in the treatment of patients with ACS.⁵ These patients are at highest risk of major adverse cardiovascular events (MACE) when compared with patients presenting with chronic coronary syndromes.⁶

IDENTIFICATION OF THE CULPRIT LESION

The focus of management for patients presenting with acute chest pain and ST elevation is immediate angiographic assessment.⁷ In the majority of patients, a culprit lesion is identified and recanalization with stenting is undertaken. However, diagnostic uncertainty can exist and the treating physician should consider non-atherosclerotic aetiologies, if presenting with atypical symptoms, unusual patient demographic/clinical risk profiles or in the

absence of significant obstructive coronary artery disease (CAD) on angiography [4-10% of patients presenting with ST elevation ACS (STEACS)^{8,9}]. The exclusion of an atherosclerotic ACS aetiology has important lifelong impacts for the patient, avoiding an erroneous diagnosis, and minimizing exposure to acute anti-thrombotic/anti-platelet and anti-atherosclerotic therapies.

Angiographic interpretation in patients with non-STEACS (NSTEMACS) poses greater challenges due to the heterogeneity of presentation with respect to time from symptom onset, electrocardiogram (ECG) changes, and the possible absence of ventricular regional wall motion abnormalities. An identifiable culprit lesion may be absent in >30% of patients and >10% of patients may have multiple culprit lesions on angiography.¹⁰ Similar to patients presenting with STEACS, 4-10% of NSTEMACS presentations have non-obstructive CAD¹¹ but associated hazard for future events.¹²

It is important to acknowledge the inherent weakness of coronary angiography to accurately assess vessel and lumen geometry, and its inability to evaluate plaque components and accurately detect the presence of thrombus – information more accurately provided by intravascular imaging.¹³ Where diagnostic or angiographic uncertainty exists in the setting of ACS, we propose a role for intracoronary imaging to aid diagnosis and guide treatment (**Figure 1**).

Intracoronary imaging can delineate luminal discontinuity/plaque disruption and associated thrombus, the hallmarks of a culprit lesion. Optical coherence tomography provides accurate detection of intraluminal thrombus¹⁴ and is capable of distinguishing red and white thrombus due to the optical attenuating property of red blood cells, abundant within red thrombus (**Figure 2** and **Supplementary Table 1**). Intravascular ultrasound detection of thrombus is more challenging (see **Figure 2**, Panel 2) but can be improved by stationary imaging at the level of the presumed thrombus and a small injection of contrast to highlight the luminal contour. The advent of high-definition IVUS promises superior resolution and improved diagnostic capabilities, however, at present a data-driven comparison with OCT is lacking.

LESION MORPHOLOGY IDENTIFICATION IN ACUTE CORONARY SYNDROME AND IMPLICATIONS FOR TREATMENT

Rupture of a thin-cap fibroatheroma (TCFA) with associated thrombus formation has been the historical focus of attention in ACS and treatment has been tailored to stabilize this plaque type.¹⁵ However, pathology series and prospective studies conducted with intracoronary imaging demonstrated that one-third of all ACS and one-quarter of STEACS are caused by plaques with an intact fibrous cap^{16,17} – the majority identified as eroded plaques and a small cohort of calcific nodules. Intravascular imaging, in particular OCT, has enabled identification of these atherothrombotic features in patients presenting with ACS, shedding light on *in vivo* mechanisms and suggesting tailored therapeutic interventions, as outlined in the subsequent sections. Despite the superior resolution of OCT, enhancing plaque identification, the presence of thrombus in the acute setting can obscure the underlying vessel wall preventing

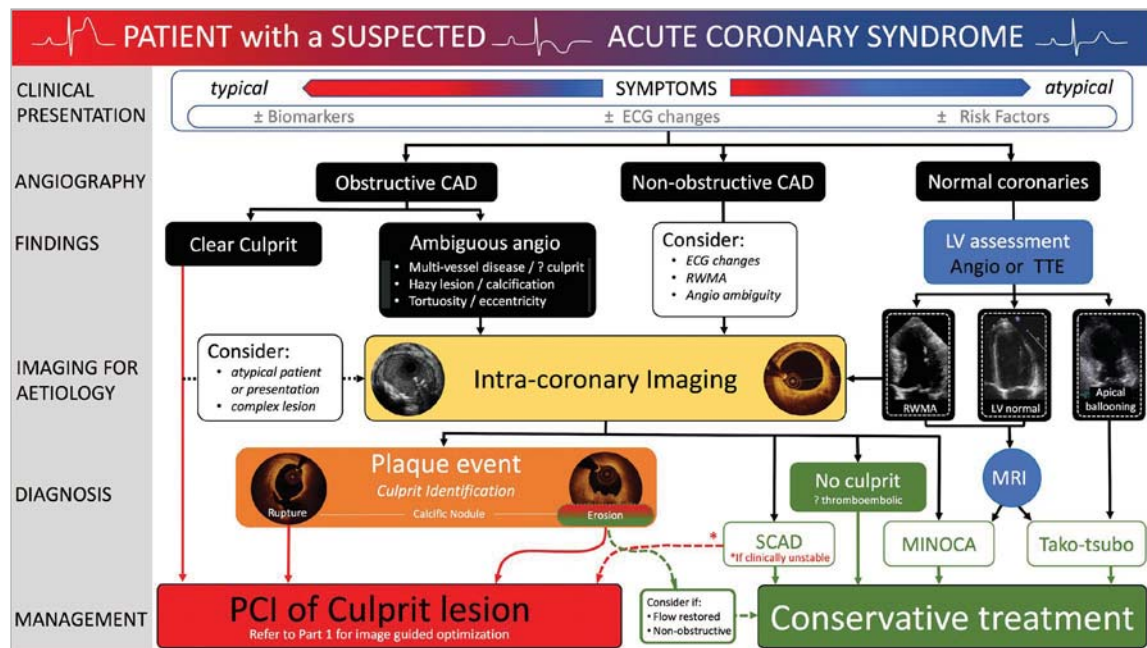


Figure 1. A treatment algorithm to guide the use of intravascular imaging in patients presenting with acute coronary syndromes.

plaque classification in >20% of cases.¹⁸ In parallel with identification of culprit plaques, intracoronary imaging has increased the awareness and diagnosis of nonatherosclerotic ACS events, discussed in Non-Atherosclerotic ACS Presentations section.

PLAQUE RUPTURE

Plaque rupture is defined by discontinuity of the fibrous cap overlying a lipid-rich core (**Figure 3**). Ruptured fibrous cap-ACS is commonly associated with a vessel wall cavity, without IVUS or OCT signal, generated through downstream embolization of the necrotic core. Thrombi are often found overlying the ruptured segment. However, thrombus may be absent at the site of an old plaque rupture or with fresh rupture treated with anti-thrombotic/anti-coagulant therapies. Multiple plaque rupture sites may be evident and differences between culprit and non-culprit lesions have been observed, with the presence of thrombus, smaller luminal area, and greater plaque burden associated with culprit lesions.¹⁹

PLAQUE EROSION

Plaque erosion is characterized by endothelial denudation, a poorly understood pathological process occurring at a level that is undetectable by current intracoronary imaging modalities. Only OCT has been successfully used, in clinical practice, to identify plaque erosion, although the diagnosis is one of exclusion, where thrombus is associated with non-disrupted plaque. An OCT diagnosis of plaque erosion is considered ‘definite’ in the absence of fibrous cap disruption, in a lesion frequently composed of fibrous tissue, with overlying luminal white thrombus. A ‘probable’ OCT-erosion may lack luminal thrombus but demonstrates an irregular luminal surface, or has overlying thrombus with attenuation of the underlying plaque, without evidence of superficial lipid or calcification in the vessel upstream or downstream of the thrombus site¹⁶

(**Figure 3**). Effective blood clearance is very important to minimize the potential for misdiagnosing OCT-erosion secondary to streaming of blood, particularly when in contact with the lumen wall.

A recent analysis of 51 patients with ACS (STE/NSTE-ACS) undergoing three-vessel OCT assessment²⁰ demonstrated that patients with erosion, vs. plaque rupture, had a lower percentage of TCFA, smaller lipid burden, and thicker fibrous cap. A large prospective series of 822 STEACS patients investigated the predictors of plaque erosion by OCT.²¹ Overall, plaque erosion tends to occur with greater frequency in younger patients, especially pre-menopausal women. Additionally, current smoking, absence of traditional coronary risk factors, lack of multi-vessel disease, reduced lesion severity, larger vessel size, and nearby bifurcation were significantly associated with plaque erosion. Nearby bifurcation and current smoking were especially notable in men, while age <50 years was most predictive in women. Existing data suggest that plaque erosion is associated with better outcomes than plaque rupture.^{22,23}

Identification of plaque erosion may facilitate tailoring of patient treatment. A proof-of-concept study, including 60 patients with short (1 month) follow-up, has demonstrated that plaque erosion associated with a residual diameter stenosis <70% may be treated conservatively, with anti-thrombotic and anti-platelet therapy, allowing avoidance of stent deployment.¹⁷ A randomized control study is needed to further explore this concept.

ERUPTIVE CALCIFIC NODULE

Discrete calcific nodule with associated plaque disruption is the least frequently observed substrate for ACS but can pose significant challenges for stent deployment and optimization. The process was first identified by IVUS²⁴ with subsequent pathological

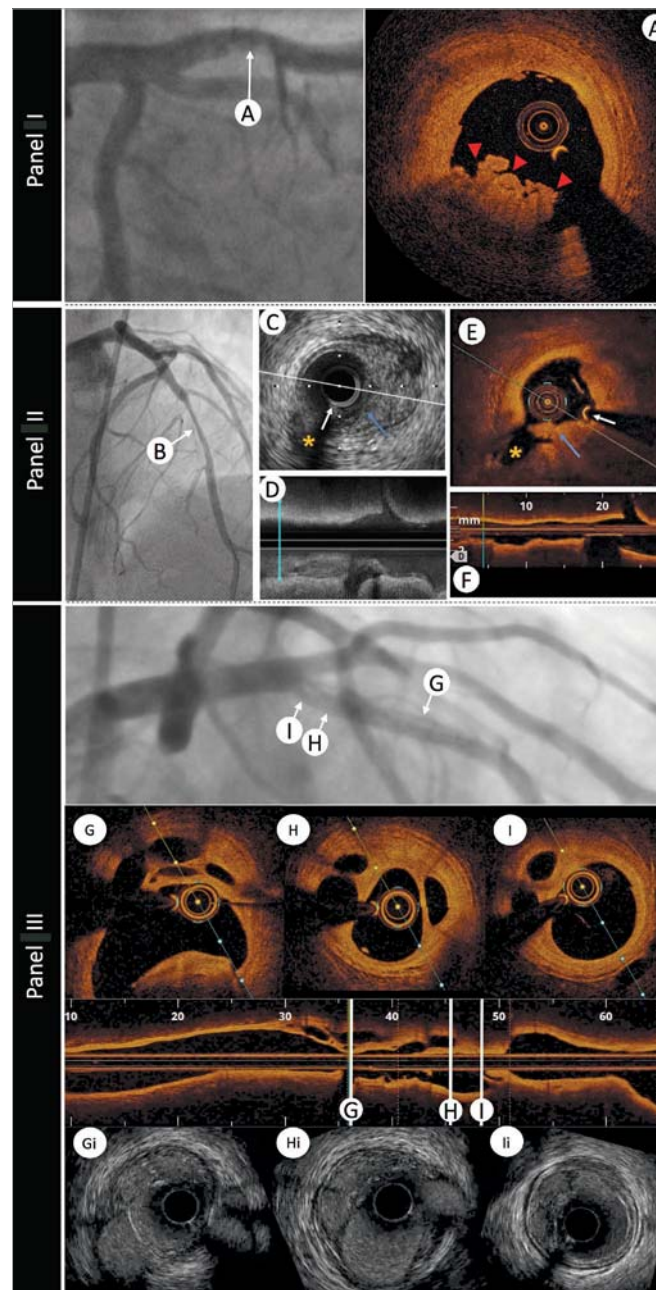


Figure 2. The role of intravascular imaging in delineating thrombus. Panel I: an angiographic image of a left anterior descending artery in a patient with ST-elevation myocardial infarction presentation and anterior ST-segment elevation. A hazy filling defect is evident in the proximal segment of the vessel, highlighted by white arrow A. Optical coherence tomography image (A) demonstrates red thrombus (red arrows) with an irregular surface and adherent to the lumen, attenuating the light, and obscuring deeper structures. Panel II: a 45-year-old woman was admitted with chest pain and anterior ST-elevation. Emergent angiography revealed a filling defect in the mid-left anterior descending artery. After thrombus aspiration angiography showed a tubular stenosis in the mid-left anterior descending artery (B) that was investigated with intracoronary imaging to determine the substrate of the acute coronary syndromes. Corresponding intravascular ultrasound and optical coherence tomography images are shown. (C and D) Cross-sectional and longitudinal intravascular ultrasound images (40 MHz) demonstrating the presence of atherosclerotic plaque (visible in C from 2 to 6). Intraluminal material protruding towards a small side branch was visible (blue arrow). Optical coherence tomography (E and F) confirmed the presence of atherosclerosis (with lipid content given the attenuation observed) and demonstrated the presence of white thrombus (irregular mass protruding into the lumen with optical shadow). White arrow indicates the guidewire artefact. Asterisk indicates the side branch used for matching of corresponding cross-sections. Panel III: left anterior descending artery with mid-vessel filling defects secondary to a conservatively managed anterior ST-elevation myocardial infarction 10 years earlier. Longitudinal optical coherence tomography imaging with three representative optical coherence tomography frames (G, H, and I) demonstrating re-canalized thrombus. Matched HD-IVUS (Boston Scientific) images (Gi, Hi, and Ii) demonstrating the superior delineation of structures with light-based imaging.

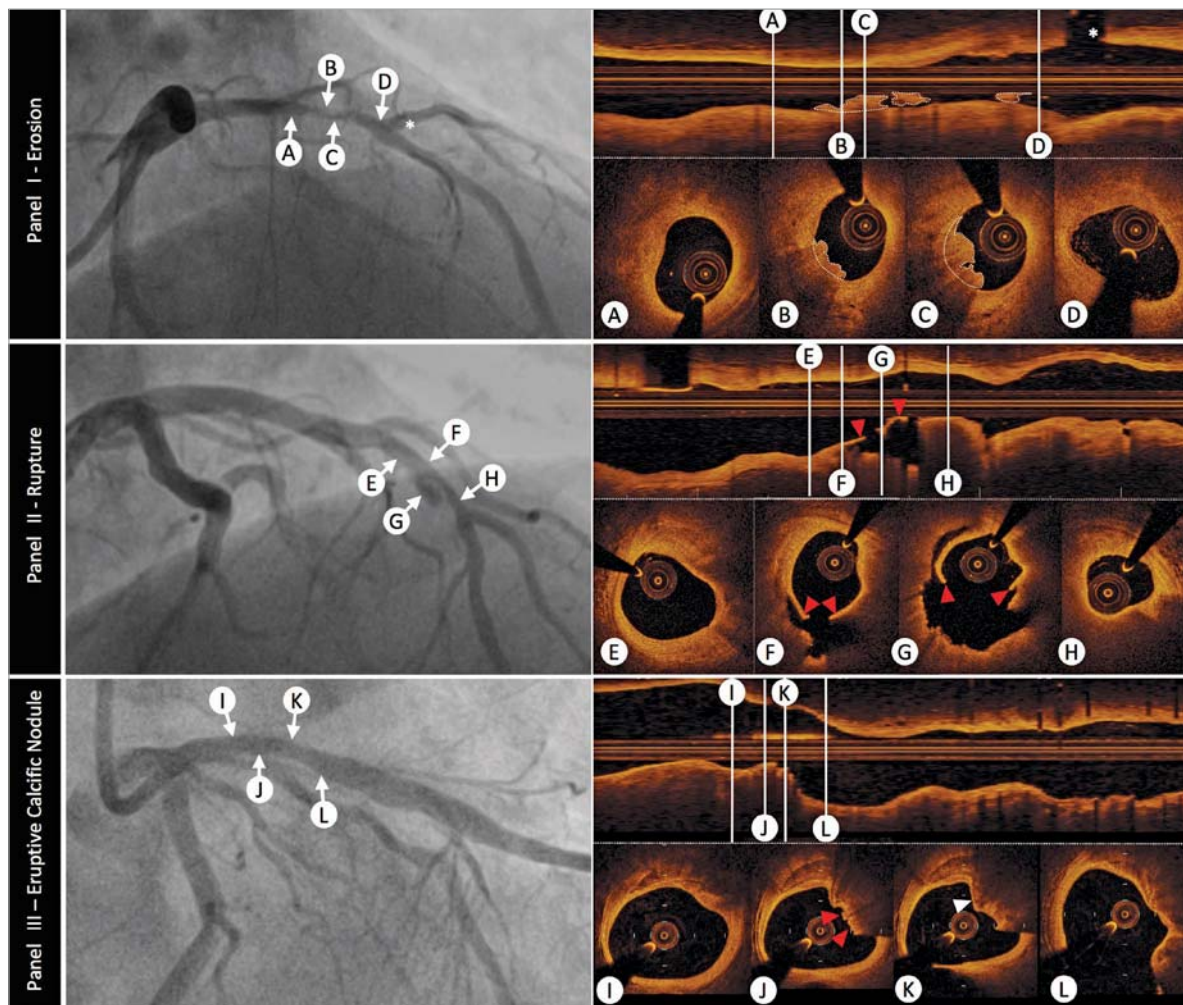


Figure 3. The role of optical coherence tomography to define atherosclerotic acute coronary syndrome plaque aetiology. Panel I: plaque erosion – angiographic image shows a severe stenosis in the mid-left anterior descending coronary artery (indicated by arrows B and C). Serial intravascular optical coherence tomography cross-sectional images indicate that no rupture is detected in the culprit lesion. Optical coherence tomography-erosion is identified as an irregular lumen surface with attached mural thrombus (white dotted outline on cross-sections and longitudinal image) overlying a fibrous plaque (B and C). Cross-sectional images indicate thick-cap fibro-atheroma proximal (A) and distal (D) to thrombus, immediately before a major diagonal branch (white asterisk). Panel II: plaque rupture – angiogram demonstrates a culprit lesion in the left anterior descending coronary artery (indicated by arrows F and G). Plaque rupture is identified on cross-sectional and longitudinal optical coherence tomography images by the disrupted fibrous-cap (red arrowheads) and a cavity formation inside the plaque (F and G). Cross-sectional images indicate optical coherence tomography-defined thin-cap fibroatheroma in the proximal (E) and distal (H) segments of the culprit lesion. Panel III: eruptive calcific nodule – angiography demonstrates a moderate lesion in the proximal left anterior descending artery (indicated by arrows J and K). Optical coherence tomography evaluation of the vessel confirms calcific infiltration of the vessel wall. The distinct margins of a superficial calcific sheet are demonstrated in Panel III-I from 11 o’clock to 2 o’clock. Disruption of the luminal contour with overlying red thrombus (red arrowheads), resulting in image attenuation (12-3 o’clock) is evident in Panel III-J. Immediately downstream the irregular protrusion of the calcific nodule is better delineated (Panel III-K white arrowhead). It is important to note that the nodule generates significant attenuation, obscuring deeper vessel structures, and this can result in misclassification as red thrombus. Endothelial integrity is confirmed more distally (Panel III-L).

studies demonstrating that eruptive calcific nodules are responsible for 2-7% of acute coronary events.²⁵ The lesions exhibit breaks in a calcified plate that disrupt the fibrous cap and are overlaid by thrombus.²⁶ Imaging of erupted calcific nodule is possible with IVUS and OCT, with OCT providing superior detection of thrombus, delineation of superficial and deep boundaries of calcium and plaque disruption (**Figure 3**). However, there are limitations to OCT

imaging, for example, the presence of protruding calcium can pose challenges in tissue differentiation, particularly through attenuation of deeper structures resulting in mis-representation as red thrombus and potential misdiagnosis of an acute culprit event. Similarly, distinguishing lipid core from calcium, if the boundaries are ill-defined, or detecting calcium when there is overlying thrombus can be better achieved with IVUS and virtual histology (VH)-IVUS.²⁷

Histopathological comparison has demonstrated that OCT can differentiate various types of coronary calcification and accurately detect calcific nodules. In clinical OCT studies, an eruptive calcific nodule has been defined as a lesion that exhibits evidence of fibrous cap discontinuity and/or thrombus, over a calcified plaque characterized by protruding calcification into the lumen, and the presence of substantive calcium proximal and/or distal to the lesion.¹⁶ Intervention in ACS patients presenting with eruptive calcific nodules is associated with higher target lesion revascularization rates, highlighting the complex nature, and challenging treatment of this lesion subset.²⁸ Recently, analysis of a large core laboratory OCT series has proposed additional calcific lesion substrate for ACS, specifically superficial calcific sheets, which were associated with greater post-PCI myocardial injury.²⁹

Delineating the nature of calcific ACS lesions with intracoronary imaging guides adjunctive therapy, including vessel preparation with aggressive pre-dilatation, cutting balloons, rotational or orbital atherectomy, laser therapy, or lithotripsy. Further studies are required to guide selection of plaque modification strategy according to calcium substrate, to ensure effective post-stent optimization, as outlined in Part 1.¹

NON-ATHEROSCLEROTIC ACUTE CORONARY SYNDROME PRESENTATIONS

Myocardial infarction with non-obstructed coronary arteries

Confirmation of non-obstructed coronaries in patients presenting with ACS is often considered a reassuring finding. However, MINOCA is not benign. Systematic review has demonstrated a 12-month mortality of 4.7%,³⁰ which far exceeds comparative rates in an equivalent population without ACS. The ESC working group on cardiovascular pharmacotherapy have outlined a differential list including angiographically undetectable plaque disruption, coronary artery spasm, coronary thromboembolism, spontaneous coronary artery dissection (SCAD), takotsubo syndrome, and myocarditis.³¹

A study of women presenting with myocardial infarction (MI) and non-obstructed coronaries revealed plaque disruption in 38% of those undergoing IVUS evaluation.³² Additionally, the superior resolution of OCT has the potential to detect a thromboembolic or vasospastic aetiology, if thrombus is observed in the absence of atherosclerosis or luminal irregularity (**Figure 4**). Clearly, the differentiation between a plaque-induced event and the presence of embolic thrombus, despite angiographically non-obstructed coronary arteries, significantly alters the acute and long-term patient management. Consequently, we advocate undertaking intracoronary imaging at the time of index angiography, if there are non-obstructive coronary lesions or if the clinical presentation does not favour other noncoronary MINOCA aetiologies (e.g. myocarditis). Usually imaging will be limited to epicardial territories with coronary lesions or associated ECG/echo features of ischaemia, however, three-vessel imaging may be considered (**Figure 1**).

Intravascular ultrasound evaluation of vasospastic coronary segments has demonstrated underlying evidence of atherosclerotic lesions with a high incidence of negative arterial remodelling³³ and

relative absence of calcium.³⁴ An OCT study, including patients presenting with ACS, demonstrated lumen irregularity with thrombus in 25% and evidence of plaque erosion in 26%, supporting the need for anti-platelet therapy in this challenging cohort.³⁵

Takotsubo syndrome was originally described in the absence of CAD but the InterTAK criteria now highlight that CAD does not exclude a diagnosis.³⁶ Intracoronary imaging is, in general, not essential for the diagnosis but may be valuable to exclude a culprit plaque event where there is evidence of angiographic atherosclerotic disease.³⁷

Spontaneous coronary artery dissection

Spontaneous coronary artery dissection is observed in 2-4% of angiograms undertaken for ACS.³⁸⁻⁴⁰ In pre-menopausal women <50 years old presenting with STEACS, the angiographic prevalence of SCAD is 10.8%.³⁹ The angiographic characteristics can vary considerably, and a classification system has been proposed.^{41,42} Type 1 represents the classical linear coronary defect with potential contrast hold-up, however, occurs in <50% cases. Type 2 defects are more commonly observed, either with an abrupt calibre reduction and subsequent normalization (Type 2a) or with persistent calibre reduction to the distal vessel (Type 2b). Spontaneous coronary artery dissection can also mimic coronary atherosclerosis (Type 3 – **Figure 4**) or simply present with abrupt vessel closure (Type 4). The findings from intravascular imaging studies have increased the interventional community's awareness of SCAD.⁴³ Intravascular imaging has provided insights into the aetiology, with evidence of separation of the intima and media from the adventitia, with or without communication with the vessel lumen⁴⁴ and can assist in confirming the diagnosis and guiding treatment.⁴⁵ However, a significant proportion of SCAD can be diagnosed angiographically, thereby limiting instrumentation of a dissected vessel that carries risks of dissection propagation and vessel closure. Therefore, when possible, a conservative treatment approach to treatment should be adopted when flow is restored.

The recent ESC/ACCA position paper on SCAD supports the role of intravascular imaging where a diagnosis by angiography is uncertain.⁴⁶ If PCI is deemed necessary due to ongoing ischaemia or clinical instability, it is important to acknowledge that there is an increased risk of procedural complications, consequently imaging may provide important guidance, in particular confirmation of the wire position in true lumen, the longitudinal extent of the vessel disruption and vessel dimensions for stent sizing, which can be problematic angiographically, in the presence of extensive intramural haematoma.

Both IVUS and OCT can be used to facilitate diagnosis of SCAD, and both modalities have strengths and weaknesses. Obvious concerns exist regarding the need for contrast injection to achieve OCT imaging, and we would advise that IVUS is preferred where there is evidence of a false lumen (Type 1), and in small calibre and tortuous vessels, where the imaging probe risks being occlusive. Additionally, the imaging penetration depth of IVUS can be advantageous in proximal vessel dissections, where the false lumen stretches the external elastic lamina, increasing the vessel size.

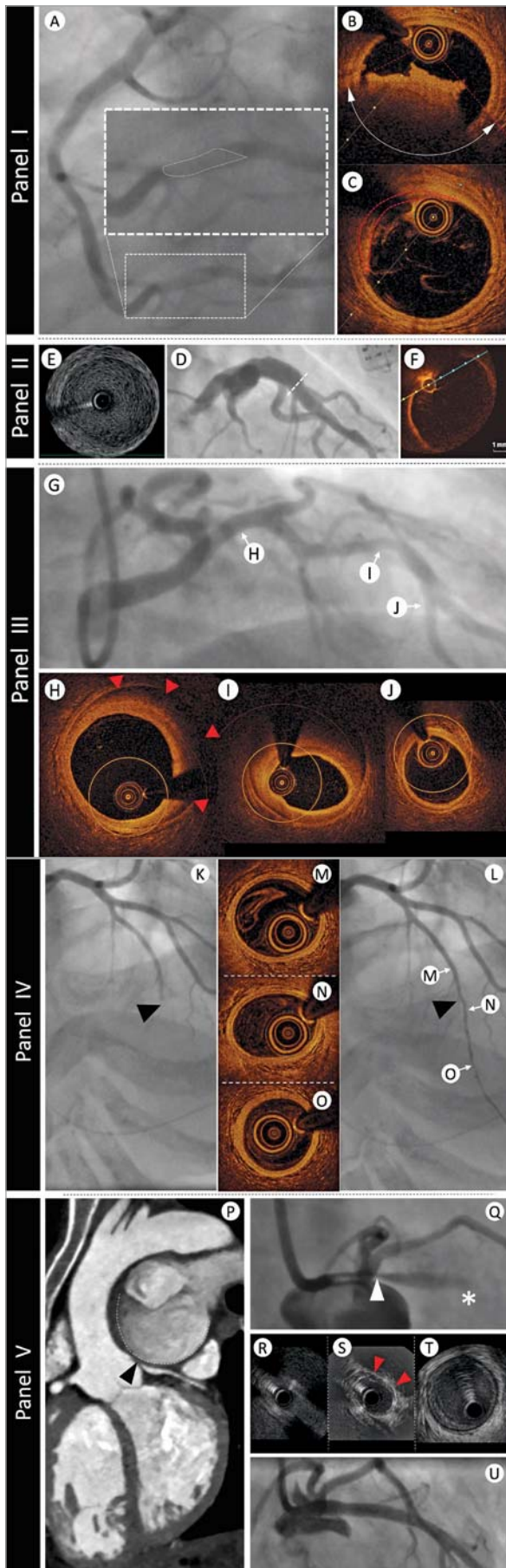


Figure 4. The role of intravascular imaging in non-atherosclerotic acute coronary syndrome presentations. **Panel I:** a 39-year-old man with no cardiovascular risk factors presented with acute onset chest and abdominal pain and evidence of inferior ST elevation. Immediate angiography demonstrated a filling defect in Segment 3 of the right coronary artery (Panel I-A - filling defect highlighted in enlarged panel by white dotted outline). Optical coherence tomography assessment confirmed fresh red thrombus with associated attenuation [Panel I-B - red dotted lines indicate margins of attenuation (white double arrow head arc)]. Neighbouring regions demonstrated minimal pathological intimal thickening with a tail of thrombus (Panel I-C - red dotted outline). The patient was commenced on a glycoprotein 2b/3a inhibitor and symptoms settled. Further evaluation of his abdominal pain revealed acute ischaemia of his small bowel secondary to thrombotic occlusion. **Panel II:** a 44-year-old man with history of childhood Kawasaki disease with coronary involvement presented with stable symptoms of angina and underwent investigation by coronary angiography. Panel II-D demonstrates proximal aneurysmal disease of the left anterior descending artery. Intravascular ultrasound evaluation (Panel II-E) highlights a large aneurysm 7 mm in diameter with minimal evidence of atheroma. The size of the aneurysm prevented accurate assessment by optical coherence tomography (Panel II-F). **Panel III:** A 39-year-old woman with a history of hypertension presented with acute onset chest pain, minor troponin elevation, and dynamic anterior t wave changes on her electrocardiogram. Angiographic assessment (Panel III-G) revealed mild-moderate calibre reduction in the mid-left anterior descending artery. Optical coherence tomography was undertaken to better delineate the nature of her angiographic abnormalities. Panel III-H demonstrates evidence of intima-medial detachment with intra-mural haematoma (red arrowheads) in a segment of the proximal left anterior descending artery that appeared angiographically normal. More extensive intramural haematoma with reduction in lumen calibre was evident at the level of the angiographic stenosis (Panel III-I). Optical coherence tomography analysis of the distal left anterior descending artery segment confirmed normal vessel architecture (Panel III-J). The patient was treated conservatively and made an excellent recovery. **Panel IV:** a 42-year-old woman without cardiovascular risk factors presented with acute onset chest pain and evidence of anterior ST elevation. Immediate angiographic assessment (Panel IV-K) revealed mid-vessel occlusion of the left anterior descending artery (black arrowhead). Passage of an 0.014" interventional guidewire resulted in recanalization of the vessel (Panel IV-L) and resolution of the ECG changes. Optical coherence tomography evaluation was undertaken to better delineate the aetiology of presentation. No significant vessel abnormalities were detected proximal (Panel IV-M), at the level of occlusion (Panel IV-N), or in the distal vessel segment (Panel IV-O). **Panel V:** a 47-year-old woman with secundum atrial septal defect and Eisenmenger's syndrome presented to an emergency department with rapidly worsening dyspnoea and palpitations. Electrocardiogram demonstrated sinus rhythm, normal repolarization, and multiple polymorphic ventricular extrasystoles. The echocardiogram showed normal left ventricle ejection fraction with only mild hypokinesia of the mid and distal anterior left ventricular wall. Immediate double rule-out computed tomography scan (Panel V-P) demonstrated extrinsic compression of the LMS (black arrowhead) from a giant pulmonary artery aneurysm (contour outlined with dashed white line). Urgent angiography (Panel V-Q) confirmed a severe ostial stenosis of the left main stem (LMS - white arrowhead) and TIMI-1 flow in the left anterior descending artery (white asterisk). A percutaneous interventional strategy was adopted and intravascular ultrasound evaluation was undertaken to appropriately size the LMS. Intravascular ultrasound confirmed dynamic compression of the LMS with complete occlusion of the ostium (Panel V-R), evidence of extrinsic compression (red arrowheads) in the shaft (Panel V-S), and normal vessel in the distal LMS segment (Panel V-T). The patient proceeded to intravascular ultrasound-guided intervention with an excellent result (Panel V-U).

However, IVUS resolution can be insufficient for the detection of intima-media complex fenestrations. Despite the vessel disruption associated with SCAD, OCT can be undertaken, where diagnostic uncertainty exists (typically Types 3 and 4) and provides greater diagnostic clarity than IVUS in assessing the distinctive features of intramural haematoma ± intimal flap^{46,47} (**Figure 1**).

ROLE OF INTRAVASCULAR IMAGING IN RISK STRATIFICATION AND VULNERABLE PLAQUE DETECTION

The term ‘vulnerable plaque’, first coined by Muller et al⁴⁸ in 1980s was used to describe plaques that are prone to rupture and caused events. Several autopsy studies have shown that the majority of ruptured plaques have a specific phenotype, namely the TCFA. This is characterized by an increased plaque burden,⁴⁹ positive remodelling, a large lipid core covered by a thin fibrous cap,⁵⁰ macrophage accumulation,⁵¹ and the presence of neovascularization.⁵²

Intravascular imaging enables *in vivo* evaluation of plaque composition and burden, identifying plaque characteristics associated with increased vulnerability. Numerous histology imaging validation studies have examined the efficacy of different invasive imaging modalities and highlighted the advantages and limitations of these techniques in assessing plaque burden, morphology, and biology⁵³ (**Supplementary Table 2**). In parallel, several prospective large-scale clinical studies have evaluated the potential value of intravascular imaging in identifying vulnerable plaques and patients who are at risk of suffering cardiovascular events.^{54,55}

INVASIVE DETECTION OF VULNERABLE PLAQUES

PROSPECT and VIVA were the first prospective studies that used three-vessel IVUS imaging to examine its efficacy in detecting nonculprit lesions that are likely to progress and cause cardiovascular events.^{54,55} In PROSPECT, a minimum lumen area $\leq 4 \text{ mm}^2$, a plaque burden $\geq 70\%$, and the presence of a TCFA phenotype, derived by VH-IVUS, were predictors of subsequent non-culprit MACE. Virtual histology defined TCFA requires $>10\%$ confluent necrotic core on three consecutive frames and an arc of necrotic core in contact with the lumen surface for $\geq 36^\circ$, reflecting the inadequate spatial resolution of IVUS to visualize thin fibrous cap.⁵⁶ Lesions with these high-risk plaque characteristics were eleven times more likely to cause events within a 3.4-year

follow-up than simple lesions [hazard ratio (HR): 11.05, 95% confidence interval (CI): 4.39-27.82; $P < 0.001$]; however, the positive predictive value of these three high-risk plaque features for subsequent events was low (18.2%).⁵⁴

The limited efficacy of VH-IVUS imaging in identifying vulnerable lesions has partially been attributed to limitations of the modality to detect plaque composition.⁵⁷ To overcome this drawback combined NIRS-IVUS imaging has been proposed. Near infrared spectroscopy imaging relies on the spectroscopic analysis of the backscattered light emitted by a NIR probe which provides information about the cholesterol content in the arterial wall. The output of this analysis is displayed in the chemogram which is a colour-coded map of the probability of the presence of lipid-rich plaques (LRPs). Lipid-rich plaques were originally defined as a lipid core $>60^\circ$ in circumferential extent with $>200 \text{ mm}$ depth and an overlying fibrous cap thickness $<450 \mu\text{m}$.⁵⁸ A measure of the lipid burden is the lipid-core burden index (LCBI): it is calculated by dividing the number of yellow pixels by the total number of pixels available, multiplied by 1000 (LCBI ranges from 0 to 1000). The $\text{LCBI}_{4\text{mm}}$ is used to quantify the maximal regions of LRP within the interventional target region, divided into 4 mm coronary segments.⁵⁹ Combining NIRS with IVUS facilitates accurate and less operator dependent detection of LRP with visualization of the lumen and plaque architecture^{57,60} (**Figure 6**). To date, there are four prospective studies demonstrating high LCBI as a strong predictor of coronary events on a patient level using either LCBI or $\text{LCBI}_{4\text{mm}}$ to predict subsequent MACE.⁶¹⁻⁶⁴

The LRP study was the first prospective large-scale imaging study that examined the efficacy of this modality in detecting vulnerable plaques on a lesion level. The study enrolled 1241 patients with stable angina (46.3%) or acute coronary syndrome (53.7%) and assessed more than 5000 lesions with NIRS-IVUS.⁶⁵ Lesion-level analysis demonstrated that the presence of LRP ($\text{LCBI}_{4\text{mm}} > 400$) was associated with a four-fold higher event rate (HR: 4.11, 95% CI: 2.3-7.34; $P < 0.001$). Also, the adjusted patient-level analysis showed that for each 100 unit increase of $\text{maxLCBI}_{4\text{mm}}$ the risk of non-culprit MACE increased by 18% and patients with $\text{maxLCBI}_{4\text{mm}}$ greater than 400 were at 87% higher risk of non-culprit MACE at 24-month follow-up.⁶⁶ Similarly, a retrospective

Box 1. Indications and clinical value of intravascular imaging in acute coronary syndromes

- Thrombus detection facilitates identification of an ACS culprit lesion.
- OCT is the current gold standard for thrombus detection.
- Intravascular imaging facilitates delineation of underlying plaque aetiology in ACS and may guide tailoring of therapy.
- When a culprit lesion, attributable to a NSTEMI presentation, is not evident angiographically, an intravascular imaging-based assessment to guide appropriate management should be considered.
- Invasive imaging evaluation in suspected SCAD should be reserved for cases where angiographic assessment is unclear (usually Types 3 and 4 or if clinical/haemodynamic instability).
- Consider intravascular imaging where there is no evidence of significant CAD, in order to characterize MINOCA.

OCT study demonstrated that OCT detected non-culprit LRP increased the risk of non-culprit MACE, with a more modest two-fold increase in risk (HR: 2.06, 95% CI: 1.05-4.04; P=0.036).⁶⁷

These studies have demonstrated the diagnostic potential but also highlighted the limitations of intravascular imaging in detecting vulnerable lesions. The complex nature of the studies led to significant levels of patient exclusion due to incomplete data and failed matching of temporal imaging (only 53% of lesions that caused events during follow-up in the PROSPECT trial were studied by IVUS at baseline). Additionally, it is important to recognize that procedural complications were reported in association with multi-vessel imaging (0.3-1.6%⁶⁷⁻⁶⁹). In the light of these limitations and an absence of data to support interventional passivation of vulnerable lesions, the routine clinical use of invasive imaging for vulnerable plaque detection cannot be recommended. Studies testing the potential value of vulnerable plaque detection (COMBINE OCT-FFR, NCT02989740; PROSPECT II, NCT02171065) and plaque sealing (PROSPECT II, NCT02171065; PREVENT, NCT02316886) are ongoing.

ROLE OF INTRAVASCULAR IMAGING IN RISK STRATIFICATION

Four prospective studies examined the potential value of intravascular imaging in identifying high-risk patients. In the ATHEROREMO-IVUS study, that included 581 patients who had coronary angiography for clinical purposes and single-vessel VH-IVUS imaging, patients that had lesions with a TCFA phenotype and an increased plaque burden (>70%) had a higher incidence of MACE at 1 year follow-up.⁷⁰ However, in this study, the event rate was low and thus it was not possible to examine whether VH-IVUS provided additional prognostic information than the well-known clinical risk factors. In addition, the LRP study and the ATHEROREMO-NIRS sub-study showed that plaque composition, and in particular an increased LCBI was associated with worse prognosis.^{63,66} Finally, in the CLIMA study (presented as a late breaking clinical trial at EuroPCR 2018) that included 1003 patients who were referred for coronary angiography and underwent OCT imaging in a non-diseased proximal left anterior descending coronary artery, the hard composite Endpoint of cardiac death and target vessel MI was 7.5× higher in patients who had lesions with a TCFA phenotype, lipid arc >180°, minimum lumen area <3.5 mm² and macrophages accumulations, compared with those with plaques without high-risk characteristics (18.9% vs. 3.0%). Non-invasive evaluation of high-risk

plaque has obvious advantages in minimizing procedural risks and has demonstrated excellent negative predictive value. However, the positive predictive value of computed tomography (CT) coronary angiography is poor, limiting its role in the prediction of acute coronary events (**Figure 5**).

Identification of high-risk/large burden plaque should trigger intensification of secondary preventative treatment, including lifestyle modification and tailoring of anti-atherosclerotic medication. However, further research is required to confirm the incremental value of intravascular imaging over clinical variables in risk stratification and subsequent treatment guidance.⁷²

Imaging of angiographically ambiguous coronary findings

Invasive coronary angiography remains the most commonly used imaging modality to assess the coronary vasculature. Angiographic ambiguity in the stable population tends to reflect excessive plaque burden (undetectable by angiography), calcification (see Part 11) old (clinically silent) plaque rupture, coronary tortuosity, or aberrant vessel anatomy. Intravascular imaging provides clarity where the angiogram demonstrates haziness, an eccentric or unexpected lesion or prevents delineation of a lesion through aneurysmal/ectatic or overlapping vessels. The availability of angiographic co-registration has facilitated reliable analysis of the intracoronary image acquisition; however, it is important to acknowledge that interpretation requires experience and expertise.

PLAQUE BURDEN

Intravascular ultrasound facilitates a thorough assessment of the entire vessel wall and demarcation of the luminal contour and external elastic lamina allows quantification of plaque burden (**Figure 6**). It requires a level of IVUS expertise to assess these plaque characteristics especially in the presence of calcific plaques that mask the external elastic lamina borders.

The highly attenuating nature of a lipid pool and necrotic core, as well as the relatively low penetration of OCT, limits its ability to visualize deeper vessel structures and consequently plaque burden cannot reliably be measured. However, work has been undertaken to find surrogates for plaque burden/vessel area with quantification of quadrants of plaque, generating a measure of plaque free wall angle. A plaque free wall angle >220° has been

Box 2. Role of imaging in vulnerable plaque detection and risk stratification

- IVUS-defined plaque burden >60-70% is predictive of subsequent MACE.
- Lipid-rich plaque (LCBI_{4mm} >400) is a predictor of plaque vulnerability and associated with a higher incidence of MACE.
- OCT and IVUS derived plaque characteristics enable identification of high-risk patients.
- Invasive plaque characterization provides superior positive predictive value of future events than CTCA.
- Identification of presumable high-risk plaque characteristics using IVUS, OCT, or NIRS-IVUS can be considered to identify high-risk patients who would benefit from an increased intensity of risk factor modification and emerging therapies targeting atherosclerosis. Prospective validation of this strategy requires confirmation.

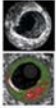
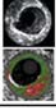
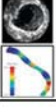
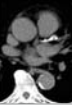
Comparison of PPV and NPV of Imaging Modality							
Study	Modality	Variables	Endpoint	Follow-up	PPV	NPV	
PROSPECT (n=697)		IVUS & VH-IVUS	PB≥70% & MLA<4mm ² & VH-IVUS TCFA	MACE (CD, cardiac arrest, MI, rehospitalization due to AP)	3 years	17%	98%
ATHEROREMO IVUS (n=581)		IVUS & VH-IVUS	PB≥70% & MLA<4mm ² & VH-IVUS TCFA	MACE (Non-CL related or indeterminate death, ACS, unplanned revascularization)	1 year	23%	93%
PREDICTION (n=506)		IVUS & ESS	PB≥58% & Low ESS<1.0Pa	PCI	1 year	41%	92%
ATHROREMO NIRS (n=203)		NIRS	maxLCBI _{4mm} >43	MACE (All-cause death, ACS, stroke, unplanned revascularisation, exclusive of event related to culprit lesion)	1 year	17%	96%
CLIMA (n=1003)		OCT	MLA<3.5mm ² & TCFA & Lipid arc >180° & Macrophage	MACE (CD and TV-MI)	1 year	19%	97%
PROMISE (n=4415)		CTA	High-risk plaque	MACE (All-cause death, MI, UAP)	2 years	6%	98%
PROMISE (n=4209)		CACS	CACS>300	MACE (All-cause death, MI, UAP)	2 years	6%	98%

Figure 5. A comparison of the positive and negative predictive values of intravascular and non-invasive imaging modalities. Summary of the positive and negative predictive values of coronary imaging-derived variables for prediction of clinical outcomes in the PROSPECT, ATHEROREMO-IVUS, PREDICTION, ATHEROREMO-NIRS, CLIMA, and PROMISE studies. AP, angina pectoris; CACS, CT angiography calcium score; CD, cardiac death; CTA, computed tomography angiography; ESS, endothelial shear stress; LCBI, lipid-core burden index; MACE, major adverse cardiac events; MI, myocardial infarction; MLA, minimal lumen area; PB, plaque burden; PCI, percutaneous coronary interventions; TCFA, thin-cap fibroatheroma; TVMI, target vessel-MI. Adapted from Koskinas et al.⁷¹

shown to predict an IVUS plaque burden <40% with PPV 78% and NPV 84%.⁷³ Similarly, quantification of LRP by OCT, with measurement of lipid arc and lipid length has been shown to predict MACE, need of revascularization and recurrent ischaemia.⁶⁷

Part 1 of the consensus document outlined the importance of delineating plaque burden to guide stent placement, aiming to avoid areas with >50% plaque burden.¹ Furthermore, both PROSPECT and the ATHEROREMO-IVUS studies have confirmed an association between the presence of plaque burden >70% in non-culprit vessels with higher MACE rates.^{70,74} Therefore, detection of plaque is important to guide optimal invasive and non-invasive treatment.

CORONARY ANEURYSMS AND ECTASIA

Defining aneurysmal or ectatic coronary segments can be challenging angiographically, especially as most recognized definitions require comparison against a 'normal' vessel segment.⁷⁵⁻⁷⁷ Consequently, recognition of aneurysmal and ectatic disease by adult cardiologists has been frequently overlooked.⁷⁸ Historical

IVUS evaluation of aneurysmal disease highlights the weakness of angiographic interpretation, as only a third of patients had the IVUS appearance of true or pseudo-aneurysmal disease. In the majority of patients the 'aneurysmal' segments represent complex plaque or normal vessel neighbouring significant stenoses.⁷⁹ Therefore, where uncertainty exists it is prudent to consider intravascular imaging to clarify the underlying vessel morphology. In aneurysms exceeding a diameter of ~5 mm, IVUS is the preferred modality due to its depth of penetration, facilitating evaluation of large vessel dimensions (**Figure 3**).

Kawasaki disease is the best described cause of coronary aneurysm and the leading cause of acquired heart disease in children in developed countries.⁸⁰ Surveillance of aneurysmal coronary disease is best achieved non-invasively⁸⁰; however, the incidence of undisclosed aneurysmal disease, discovered at the time of coronary angiography, has a reported rate of 3-5%.^{78,81} Kawasaki disease patients may present with ischaemic symptoms precipitated by the development of stenoses at the outlet of aneurysms or

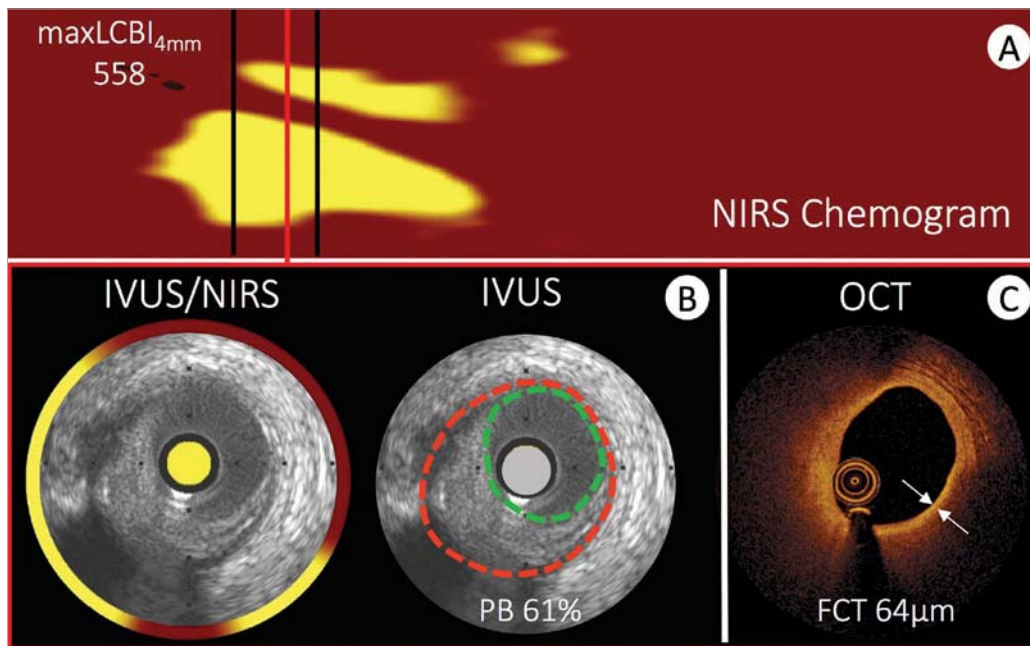


Figure 6. Intravascular imaging evaluation of a high-risk coronary plaque. An example of high-risk coronary plaque evaluated using all three available intravascular imaging modalities. (A) A near infrared spectroscopy chemogram of a bystander vessel segment in a patient presenting with acute myocardial infarction. Yellow areas represent lipid and the region between the black lines highlight the region with a maximal lipid-core burden index of 558. Matched cross-sectional images from intravascular ultrasound to near infrared spectroscopy, greyscale intravascular ultrasound (B) and optical coherence tomography (C) highlight the differences in vessel evaluation with each modality. The circumferential near infrared spectroscopy output highlights lipid signal extending from 4 o'clock to 11 o'clock (interrupted by guidewire artefact at 6 o'clock). The intravascular ultrasound greyscale image facilitates assessment of plaque burden (EEM: red, lumen: green), which amounts to 61%. Optical coherence tomography (C) of the same plaque shows the fibrous cap as a signal rich luminal layer from 3 o'clock to 12 o'clock and a light attenuating signal poor region behind. The fibrous cap thickness amounts to 64 μ m. All methods are consistent with a lipid rich fibroatheroma and optical coherence tomography in addition indicates the presence of a thin cap fibroatheroma.

giant aneurysm thrombosis.⁸² Intervention in these patients can be challenging due to calcification of the aneurysm and difficulties in assessing the true luminal dimensions,⁸³ and the use of IVUS should be considered to guide intervention.⁸⁰

AORTO-OSTIAL AMBIGUITY

The aorto-ostial junction is a unique segment of the coronary arterial tree and provides both diagnostic and interventional challenges. The angle of take-off of the proximal coronary vessels, from the aorta, can result in the angiographic appearance of a significant stenosis and functional assessment may be difficult to perform. For these reasons, morphological assessment [confirmation of atherosclerotic disease/assessment of the minimal lumen area (MLA) (see Role of Intravascular Imaging for Assessment of Lesion Severity section)] should be considered to better determine the ischaemic potential. Furthermore, the aorto-ostial position offers unique tissue characteristics with greater amounts of elastic tissue increasing the risk of stent recoil and subsequent failure.⁸⁴ Achieving a blood-free field for imaging is challenging in aorto-ostial lesions, consequently IVUS is recommended. Co-axial positioning and disengagement of the guide minimizes over-estimation of the MLA or mis-interpretation of true ostial disease, respectively.⁸⁵

Angiographic assessment can also be impacted by the anomalous take-off of the coronary vessels or extrinsic compression. There are many patterns of coronary artery anomaly, however, a 'malignant course' at risk of ischaemia or sudden cardiac death is associated with an inter-arterial course (i.e. between the aorta and pulmonary artery).⁸⁶ Most often these anomalies are discovered incidentally in later life, with increasing frequency now that CT angiography is widely used.⁸⁷ Occasionally younger patients with syncope or angina may require confirmation of the flow limiting potential of the compressive mechanism.⁸⁸ IVUS may be useful to confirm extrinsic compression and a slit-like lumen. Coronary compression can also result from dilatation of the pulmonary artery due to pulmonary hypertension,⁸⁹ acute aortic dissection,⁹⁰ or following heart surgery⁹¹ and invasive imaging may be required to provide diagnostic clarity (Figure 4).

TRANSPLANT VASCULOPATHY

Cardiac allograft vasculopathy (CAV) is a leading cause of long-term mortality after heart transplantation. Routine surveillance for CAV is necessary to ensure early diagnosis, as patients are frequently asymptomatic due to allograft denervation. Although non-invasive imaging of the coronaries can be achieved with CT, there

are limitations that prevent visualization of the distal vascular bed and image quality can be degraded by high resting heart rates.⁹² Coronary angiography remains the preferred screening tool for CAV but the diffuse, concentric nature of vasculopathy, combined with positive remodelling, can lead to a failure to diagnose CAV or an underestimation of disease severity. Intravascular imaging allows cross-sectional evaluation of the vessel wall and IVUS has been shown to provide prognostic information, with progression of intimal thickening ≥ 0.5 mm from baseline to 1 year associated with non-fatal MACE.⁹³ Furthermore, VH-IVUS can provide further characterization of CAV.⁹⁴ Consistent with findings in native CAD, IVUS-defined attenuated plaque has been shown to be associated with an increased event rate and is predictive of rejection.⁹⁵ OCT offers higher resolution and initial experience suggests it will provide early detection of CAV and offer insights into the mechanisms underlying the process.^{96,97} The European Association of Cardiovascular Imaging recommends that IVUS is used in conjunction with angiography, where expertise is available, with a baseline study undertaken to assess for donor heart CAD and at 1 year after transplantation to detect rapidly progressive CAV⁹⁸ and guide changes to immunosuppressive therapy.

Role of intravascular imaging for assessment of lesion severity

Percutaneous coronary intervention for stable angina is indicated for haemodynamically significant coronary stenoses with insufficient response to optimized medical therapy and/or the improvement of prognosis through treatment of proximal major epicardial coronary disease, multi-vessel disease with impaired left ventricular (LV) function, last remaining vessel, or the presence of significant ischaemia (involving $>10\%$ of LV mass).⁵ The limitations of coronary angiography, for delineating the true nature/extent of coronary atheroma, have already been outlined in Part 1.¹ Pressure-derived invasive indices of coronary lesion significance have been accepted as the gold standard method of invasive ischaemia assessment, with a Class I, Level of evidence A, recommendation for the use of fractional flow reserve (FFR),^{5,99-101} or instantaneous wave free ratio (iFR).^{102,103} Attempts have been made, through comparison with FFR, to identify imaging-based vessel/lesion measurements

predictive of ischaemia. Minimal lumen area is the intravascular imaging metric used to define flow-limiting stenoses; however, it has limitations to identify a single cut-off measurement due to variations in patient body mass, heart weight, lesion complexity, and the territory of ischaemic potential. Despite these limitations, in many cases intravascular imaging can detect significant stenoses overlooked by angiography or exclude pseudo-narrowings falsely detected angiographically. The limitations of pressure-derived functional indices for the assessment of left main lesion severity and the proven value of IVUS to guide PCI suggest a liberal diagnostic application.

MINIMAL LUMEN AREA AS A PREDICTOR OF ISCHAEMIC POTENTIAL IN LEFT MAIN LESIONS

Interpretation of left main coronary artery (LMCA) disease requires special attention due to its prognostic importance. The aorto-ostial and distal branching pattern of the vessel often makes assessment of lesion significance challenging,¹⁰⁴ and the interventional cardiologist must balance the need for confirmation of ischaemia with pressure-derived assessment vs. an improved understanding of the anatomical characteristics of the lesion. Ideally, use of both FFR and intravascular imaging would provide a comprehensive assessment of a LMCA lesion but in the real world the equipment costs and time constraints limit this strategy. Additionally, physiological evaluation of the LMCA can be challenging, especially in ostial stenosis or situations with concomitant disease in the left anterior descending artery or LCX, and clinical trial data supporting its use in this specific setting is scant. Consequently, the use of imaging-derived measurements to predict ischaemia can offer benefits for the rationalization of procedural time and costs and was given a Class IIa recommendation in the most recent ESC guidelines on myocardial revascularization.⁵

The proximal nature of the LMCA segment limits the variability of its calibre and anatomy, minimizing the impact of body mass and heart size on vessel and lesion measurements, however, a population variation in the LMCAMLA cut-off has been observed.¹⁰⁵ An Asian study of IVUS-derived MLA detected a cut-off of 4.5 mm^2 , correlating with an $\text{FFR} \leq 0.80$ ¹⁰⁶; however, a previous US study observed that an IVUS MLA $<5.9 \text{ mm}^2$ has the best correlation with

Box 3. Consensus recommendation on the role of imaging to assess lesion significance

- Pressure-derived haemodynamic assessment is the gold standard for deferring revascularization in patients with non-LMCA stable coronary artery disease.
- LMCA sizing demonstrates less variability than other major epicardial vessels and cut-off values of $\text{MLA} <6 \text{ mm}^2$ and $<4.5 \text{ mm}^2$ to predict functional impact have been validated with IVUS, in Western and Asian populations, respectively.
- LMCA IVUS-derived $\text{MLA} >6 \text{ mm}^2$ can be considered non-ischaemic.
- LMCA IVUS-derived $\text{MLA} \leq 4.5 \text{ mm}^2$ can be considered ischaemia generating.
- LMCA IVUS-derived $\text{MLA} 4.5\text{--}6 \text{ mm}^2$ suggests that additional invasive or non-invasive assessments of ischaemia are advisable.
- MLA measurement of non-LMCA lesions is not recommended for the assessment of lesion significance due to variations according to vessel calibre and subtended myocardium.

an FFR <0.75 (sensitivity 93% and specificity 94%).¹⁰⁷ The average MLA in patients recruited to these studies differed by 2.8 mm² (4.8 vs. 7.6 mm², respectively). In addition to the geographical differences in LMCA size, IVUS has also demonstrated differences in the characteristics of LMCA disease, with a greater burden of atheroma but less calcification in Asian LMCA lesions.¹⁰⁸

In a prospective application of the MLA cut-off, the LITRO study guided LMCA PCI by IVUS criteria and 6 mm² was found to have the highest sensitivity and specificity for detecting ischaemia.¹⁰⁹ At 2 years, the outcome of deferred patients was equivalent to that of the revascularized group. Importantly, the outcome of the few patients with LMCA MLA <6 mm² that did not undergo revascularization was significantly worse. Consequently, it appears reasonable to defer LMCA revascularization if the MLA > 6 mm², to intervene if the MLA <4.5 mm² and to consider further evaluation with FFR if the MLA is between 4.5 and 6 mm², with appropriate consideration of associated comorbidities (Figure 7). The additional advantages to intracoronary imaging-guided LMCA intervention have been addressed in the Part 1 document and includes the ability to reveal pseudo-stenoses at the ostium due to ostial spasm, incomplete vessel filling due to streaming and poor catheter alignment.

Limited data exists supporting the use of OCT for guidance of left main intervention and is not recommended for evaluation of ostial disease or short left main stems. Importantly, the MLA cut-off values established for IVUS assessment of the LMCA cannot be directly translated to OCT.

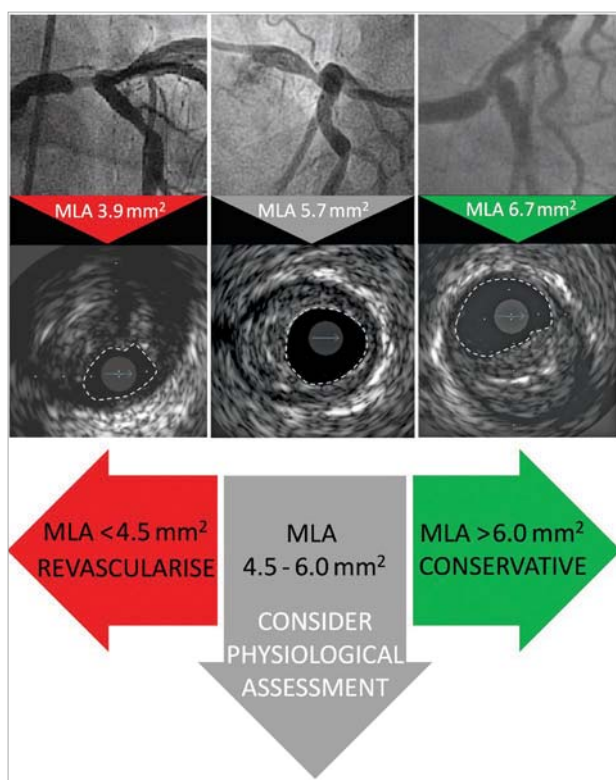


Figure 7. A schematic representation of the role of minimal lumen area assessment in the evaluation of left main coronary disease.

MINIMAL LUMEN AREA AS A PREDICTOR OF ISCHAEMIC POTENTIAL IN NON-LEFT MAIN LESIONS

Beyond LMCA disease, the variations in patient body mass, vessel calibre, and the subtended myocardium prevent the use of a single MLA cut-off value to define ischaemic potential and guide appropriate intervention. A meta-analysis of >2500 patients confirmed modest diagnostic accuracy for both IVUS and OCT for identification of haemodynamically significant lesions, with marked differences in the median cut-off values for both modalities [1.96 mm² (1.85-1.98 mm²) for OCT and 2.9 mm² (2.7-3.1 mm²) for IVUS (area under the curve 0.80 and 0.77, respectively)].¹¹⁰ Similar to the LMCA MLA assessment, a geographical variation has been observed with smaller measurements reported in Asian studies. Direct comparison of OCT, IVUS, and FFR has been reported and demonstrated slight superiority of OCT over IVUS, specifically in smaller vessels (<3 mm) secondary to better delineation of the luminal area.^{111,112} We recommend the use of pressure-derived assessment of lesion significance, but acknowledge that evaluation of the MLA data may assist in decision-making where intracoronary imaging has been used.

Conclusion

Since the publication of Part 1 of the expert consensus, the ESC guidelines committee has acknowledged the results of randomized trials comparing OCT with angiography- and IVUS-guided PCI and elevated the recommendation for use of OCT in stent optimization from Class IIb to IIa.² Furthermore, the first all-comers study of IVUS vs. angiography-guided PCI, appropriately powered to demonstrate clinical superiority, has reported, clearly favouring an imaging-guided approach.³ With an increasing complexity of both patient comorbidity and CAD, considered for percutaneous revascularization, the role of intravascular imaging to guide PCI optimization and improve longterm outcomes will continue to grow. Part 2 has outlined additional indications for the use of intravascular imaging to overcome some of the limitations posed by invasive coronary angiography. As yet, evidence from dedicated clinical trials to support many of these potential uses is lacking but among the community of imaging experts it is believed that intravascular imaging will facilitate a tailored approach to PCI for patients at high risk of recurrent events and stent failure.¹¹³ Continued advancements in the technology, with higher resolution, faster image acquisition times, combined OCT/IVUS catheters, and more sophisticated coregistered image analysis, will facilitate greater adoption through ease of use and interpretation. Intracoronary imaging-guided PCI has an exciting future.

Conflict of interest

Thomas W. Johnson reports personal fees from Abbott Vascular, Astra Zeneca, Bayer Healthcare, Boston Scientific, Daiichi Sankyo, and Terumo Inc. Lorenz Räber reports personal fees from Abbott Vascular, Amgen, Astra Zeneca, Biotronik, and Sanofi Aventis;

grants from Abbott Vascular and Sanofi Aventis. Carlo di Mario reports personal fees from Volcano; grants from Abbott, Medtronic and Shockwave. Alessio Mattesini reports grants from Shockwave Medical Inc. Nieves Gonzalo reports personal fees from Abbott and Boston Scientific. Jose M. de la Torre Hernandez reports personal fees from Abbott Laboratories, Boston Scientific, and Medtronic; grants from Amgen Inc. and Bristol Myers Squibb. Francesco Prati reports personal fees from Amgen and St. Jude Medical; grants from Bayer AG. Konstantinos Koskinas reports personal fees from Amgen and Sanofi Aventis. Michael Joner reports personal fees from Biotronik and Orbus Neich; grants from Biotronik, Boston Scientific, and Edwards Lifesciences. Maria D. Radu reports personal fees from Abbott. David Erlinge reports personal fees from Astra Zeneca; grant fees from Bayer. Evelyn Regar reports grants from Abbott Vascular. Vijay Kunadian reports personal fees from Bayer; grants from Astra Zeneca. Akiko Maehara reports personal and grant fees from Abbott Vascular and Boston Scientific. Robert A. Byrne reports personal fees from B. Braun, Biotronik, Boston Scientific, and Micell Technologies; grants from Boston Scientific and Celonova. Davide Capodanno reports personal fees from Abbott, Astra Zeneca, Bayer, Cordis, and Daiichi Sankyo. Takashi Akasaka reports personal fees from Abbott Vascular, Amgen, Astellas, Bayer, Boehringer-Ingelheim, Boston Scientific, Chugai Pharma Japan, Daiichi Sankyo, Eisai, Goodman Japan Ltd., Heartflow Japan G.K., Medtronic, Mochida Pharmaceutical Co. Ltd., MSD, Novartis, Pfizer, Otsuka Pharmaceutical Co. Ltd., St. Jude Medical, Shionogi, Sumitomo Dainippon Pharma, Takeda Pharmaceuticals, Terumo Inc., Toa Elyo Ltd., and Volcano; and grants from Abbott Vascular, Astellas, Boehringer-Ingelheim, Boston Scientific, Daiichi Sankyo, Heartflow, Otsuka Pharmaceutical Co. Ltd., Mebix, Nippon Shinyaku Co. Ltd. MSD, Terumo Inc., Toa Elyo Ltd., and Volcano. William Wijns reports personal fees from Biotronik and Microport. Gary S. Mintz reports personal fees from Boston Scientific and Philips; grants from Abbott Vascular and Boston Scientific. Giulio Guagliumi reports personal fees and grants from Abbott and Boston Scientific. Christos Bourantas and Haibo Jia have nothing to disclose.

Appendix. Authors' affiliations

1. Department of Cardiology, Bristol Heart Institute, University Hospitals Bristol NHSFT & University of Bristol, BS2 8HW, Bristol, United Kingdom; 2. Department of Cardiology, Bern University Hospital, University of Bern, Bern, Switzerland; 3. Structural Interventional Cardiology, Careggi University Hospital, Florence, Italy; 4. Department of Cardiology, Barts Heart Centre, Barts Health NHS & Queen Mary University, London, United Kingdom; 5. Department of Cardiology, 2nd Affiliated Hospital of Harbin Medical University, The Key Laboratory of Myocardial Ischemia, Chinese Ministry of Education, Harbin, China; 6. Department of Cardiology, Instituto Cardiovascular, Hospital Clínico San Carlos, Madrid, Spain; 7. Department of Cardiology, Hospital Universitario Marques de Valdecilla, IDIVAL, Santander, Spain; 8. Department of Cardiology, San Giovanni Hospital, Rome, Italy & CLI Foundation

Rome, Italy; 9. Deutsches Herzzentrum München, DZHK (German Center for Cardiovascular Research), Partner Site Munich Heart Alliance, Technische Universität München, Munich, Germany; 10. Department of Cardiology, The Heart Center, Rigshospitalet, Copenhagen University Hospital, Copenhagen, Denmark; 11. Department of Cardiology, Lund University, Skane University Hospital, Lund, Sweden; 12. Department of Cardiovascular Surgery, Zürich University Hospital, Zürich, Switzerland; 13. Institute of Cellular Medicine, Newcastle University and Cardiothoracic Centre, Freeman Hospital, Newcastle upon Tyne NHS Foundation Trust, Newcastle upon Tyne, United Kingdom; 14. Cardiovascular Research Foundation, Columbia University, New York, NY, USA; 15. Division of Cardiology, Cardio-Thoraco-Vascular and Transplant Department, CAST, Rodolico Hospital, AOU "Policlinico-Vittorio Emanuele", University of Catania, Catania, Italy; 16. Wakayama Medical University, Wakayama, Japan; 17. The Lambe Institute for Translational Medicine and Curam, National University of Ireland Galway, Saolta University Healthcare Group, Galway, Ireland; 18. Cardiovascular Department, Ospedale Papa Giovanni XXIII, Bergamo 24127, Italy.

References

- Räber L, Mintz GS, Koskinas KC, Johnson TW, Holm NR, Onuma Y, Radu MD, Joner M, Yu B, Jia H, Meneveau N, de la Torre Hernandez JM, Escaned J, Hill J, Prati F, Colombo A, di Mario C, Regar E, Capodanno D, Wijns W, Byrne RA, Guagliumi G; ESC Scientific Document Group. Clinical use of intracoronary imaging. Part 1: guidance and optimization of coronary interventions. An expert consensus document of the European Association of Percutaneous Cardiovascular Interventions. *Eur Heart J*. 2018;39:3281-3300.
- Neumann F-J, Sousa-Uva M, Ahlsson A, Alfonso F, Banning AP, Benedetto U, Byrne RA, Collet J-P, Falk V, Head SJ, Juni P, Kastrati A, Koller A, Kristensen SD, Niebauer J, Richter DJ, Seferovic PM, Sibbing D, Stefanini GG, Windecker S, Yadav R, Zembala MO; ESC Scientific Document Group. 2018 ESC/EACTS Guidelines on myocardial revascularization. *Eur Heart J*. 2019;40:87-165.
- Zhang J, Gao X, Kan J, Ge Z, Han L, Lu S, Tian N, Lin S, Lu Q, Wu X, Li Q, Liu Z, Chen Y, Qian X, Juan W, Chai D, Chen C, Li X, Gogas BD, Pan T, Shan S, Ye F, Chen S-L. Intravascular ultrasound-guided versus angiography-guided implantation of drug-eluting stent in all-comers: the ULTIMATE trial. *J Am Coll Cardiol*. 2018;72:3126-37.
- di Mario C, Koskinas KC, Räber L. Clinical benefit of IVUS guidance for coronary stenting: the ULTIMATE step toward definitive evidence? *J Am Coll Cardiol*. 2018;72:3138-41.
- Neumann FJ, Sousa-Uva M, Ahlsson A, Alfonso F, Banning AP, Benedetto U, Byrne RA, Collet JP, Falk V, Head SJ, Juni P, Kastrati A, Koller A, Kristensen SD, Niebauer J, Richter DJ, Seferovic PM, Sibbing D, Stefanini GG, Windecker S, Yadav R, Zembala MO; ESC Scientific Document Group. 2018 ESC/EACTS Guidelines on myocardial revascularization. *Eur Heart J*. 2018;40:87-165.
- Pilgrim T, Vranckx P, Valgimigli M, Stefanini GG, Piccolo R, Rat J, Rothenbuhler M, Stortecky S, Raber L, Blochlinger S, Hunziker L, Silber S, Juni P, Serruys PW, Windecker S. Risk and timing of recurrent ischemic events among patients with stable ischemic heart disease, non-ST-segment elevation acute coronary syndrome, and ST-segment elevation myocardial infarction. *Am Heart J*. 2016;175:56-65.
- Ibanez B, James S, Agewall S, Antunes MJ, Bucciarelli-Ducci C, Bueno H, Caforio ALP, Crea F, Goudevanos JA, Halvorsen S, Hindricks G, Kastrati A, Lenzen MJ, Prescott E, Roffi M, Valgimigli M, Varenhorst C, Vranckx P,

- Widimsky P; ESC Scientific Document Group. 2017 ESC Guidelines for the management of acute myocardial infarction in patients presenting with ST-segment elevation: the Task Force for the management of acute myocardial infarction in patients presenting with ST-segment elevation of the European Society of Cardiology (ESC). *Eur Heart J*. 2018;39:119-77.
8. Andersson HB, Pedersen F, Engström T, Helqvist S, Jensen MK, Jørgensen E, Kelbæk H, Råder SBEW, Saunamäki K, Bates E, Grande P, Holmvang L, Clemmensen P. Long-term survival and causes of death in patients with STElevation acute coronary syndrome without obstructive coronary artery disease. *Eur Heart J*. 2018;39:102-10.
9. Larsen AI, Nilsen DW, Yu J, Mehran R, Nikolsky E, Lansky AJ, Caixeta A, Parise H, Fahy M, Cristea E, Witzembichler B, Guagliumi G, Peruga JZ, Brodie BR, Dudek D, Stone GW. Long-term prognosis of patients presenting with ST-segment elevation myocardial infarction with no significant coronary artery disease (from the HORIZONS-AMI trial). *Am J Cardiol*. 2013;111:643-8.
10. Kerensky RA, Wade M, Deedwania P, Boden WE, Pepine CJ. Revisiting the culprit lesion in non-Q-wave myocardial infarction. *J Am Coll Cardiol*. 2002;39:1456-63.
11. Gehrle ER, Reynolds HR, Chen AY, Neelon BH, Roe MT, Gibler WB, Ohman EM, Newby LK, Peterson ED, Hochman JS. Characterization and outcomes of women and men with non-ST-segment elevation myocardial infarction and nonobstructive coronary artery disease: results from the Can Rapid Risk Stratification of Unstable Angina Patients Suppress Adverse Outcomes with Early Implementation of the ACC/AHA Guidelines (CRUSADE) quality improvement initiative. *Am Heart J*. 2009;158:688-94.
12. Kang WY, Jeong MH, Ahn YK, Kim JH, Chae SC, Kim YJ, Hur SH, Seong IW, Hong TJ, Choi DH, Cho MC, Kim CJ, Seung KB, Chung WS, Jang YS, Rha SW, Bae JH, Cho JG, Park SJ; Korea Acute Myocardial Infarction Registry Investigators. Are patients with angiographically near-normal coronary arteries who present as acute myocardial infarction actually safe? *Int J Cardiol*. 2011;146:207-12.
13. Nissen SE, Gurley JC, Grines CL, Booth DC, McClure R, Berk M, Fischer C, DeMaria AN. Intravascular ultrasound assessment of lumen size and wall morphology in normal subjects and patients with coronary artery disease. *Circulation*. 1991;84:1087-99.
14. Kubo T, Imanishi T, Takarada S, Kuroi A, Ueno S, Yamano T, Tanimoto T, Matsuo Y, Masho T, Kitabata H, Tsuda K, Tomobuchi Y, Akasaka T. Assessment of culprit lesion morphology in acute myocardial infarction: ability of optical coherence tomography compared with intravascular ultrasound and coronary angiography. *J Am Coll Cardiol*. 2007;50:933-9.
15. Falk E, Nakano M, Bentzon JF, Finn AV, Virmani R. Update on acute coronary syndromes: the pathologists' view. *Eur Heart J*. 2013;34:719-28.
16. Jia H, Abtahian F, Aguirre AD, Lee S, Chia S, Lowe H, Kato K, Yonetsu T, Vergallo R, Hu S, Tian J, Lee H, Park SJ, Jang YS, Raffel OC, Mizuno K, Uemura S, Itoh T, Kakuta T, Choi SY, Dauerman HL, Prasad A, Toma C, McNulty I, Zhang S, Yu B, Fuster V, Narula J, Virmani R, Jang IK. In vivo diagnosis of plaque erosion and calcified nodule in patients with acute coronary syndrome by intravascular optical coherence tomography. *J Am Coll Cardiol*. 2013;62:1748-58.
17. Jia H, Dai J, Hou J, Xing L, Ma L, Liu H, Xu M, Yao Y, Hu S, Yamamoto E, Lee H, Zhang S, Yu B, Jang I-K. Effective anti-thrombotic therapy without stenting: intravascular optical coherence tomography-based management in plaque erosion (the EROSION study). *Eur Heart J*. 2017;38:792-800.
18. Guagliumi G, Capodanno D, Saia F, Musumeci G, Tarantini G, Garbo R, Tumminello G, Sirbu V, Coccato M, Fineschi M, Trani C, De Benedictis M, Limbruno U, De Luca L, Niccoli G, Bezerra H, Ladich E, Costa M, Biondi Zoccai G, Virmani R; OCTAVIA Trial Investigators. Mechanisms of atherothrombosis and vascular response to primary percutaneous coronary intervention in women versus men with acute myocardial infarction: results of the OCTAVIA study. *JACC Cardiovasc Interv*. 2014;7:958-68.
19. Tian J, Ren X, Vergallo R, Xing L, Yu H, Jia H, Soeda T, McNulty I, Hu S, Lee H, Yu B, Jang IK. Distinct morphological features of ruptured culprit plaque for acute coronary events compared to those with silent rupture and thin-cap fibroatheroma: a combined optical coherence tomography and intravascular ultrasound study. *J Am Coll Cardiol*. 2014;63:2209-16.
20. Sugiyama T, Yamamoto E, Bryniarski K, Xing L, Lee H, Isobe M, Libby P, Jang IK. Nonculprit plaque characteristics in patients with acute coronary syndrome caused by plaque erosion vs plaque rupture: a 3-vessel optical coherence tomography study erosion vs rupture nonculprit plaque morphology in acute coronary syndrome erosion vs rupture nonculprit plaque morphology in acute coronary syndrome. *JAMA Cardiol*. 2018;3:207-14.
21. Dai J, Xing L, Jia H, Zhu Y, Zhang S, Hu S, Lin L, Ma L, Liu H, Xu M, Ren X, Yu H, Li L, Zou Y, Zhang S, Mintz GS, Hou J, Yu B. In vivo predictors of plaque erosion in patients with ST-segment elevation myocardial infarction: a clinical, angiographical, and intravascular optical coherence tomography study. *Eur Heart J*. 2018;39:2077-85.
22. Yonetsu T, Lee T, Murai T, Suzuki M, Matsumura A, Hashimoto Y, Kakuta T. Plaque morphologies and the clinical prognosis of acute coronary syndrome caused by lesions with intact fibrous cap diagnosed by optical coherence tomography. *Int J Cardiol*. 2016;203:766-74.
23. Niccoli G, Montone RA, Di Vito L, Gramegna M, Refaat H, Scalone G, Leone AM, Trani C, Burzotta F, Porto I, Aurigemma C, Prati F, Crea F. Plaque rupture and intact fibrous cap assessed by optical coherence tomography portend different outcomes in patients with acute coronary syndrome. *Eur Heart J*. 2015;36:1377-84.
24. Duissailant GR, Mintz GS, Pichard AD, Kent KM, Satler LF, Popma JJ, Griffin J, Leon MB. Intravascular ultrasound identification of calcified intraluminal lesions misdiagnosed as thrombi by coronary angiography. *Am Heart J*. 1996;132:687-9.
25. Virmani R, Kolodgie FD, Burke AP, Farb A, Schwartz SM. Lessons from sudden coronary death: a comprehensive morphological classification scheme for atherosclerotic lesions. *Arterioscler Thromb Vasc Biol*. 2000;20:1262-75.
26. Virmani R, Burke AP, Farb A, Kolodgie FD. Pathology of the vulnerable plaque. *J Am Coll Cardiol*. 2006;47:C13-C18.
27. Sawada T, Shite J, Garcia-Garcia HM, Shinke T, Watanabe S, Otake H, Matsumoto D, Tanino Y, Ogasawara D, Kawamori H, Kato H, Miyoshi N, Yokoyama M, Serruys PW, Hirata K. Feasibility of combined use of intravascular ultrasound radiofrequency data analysis and optical coherence tomography for detecting thin-cap fibroatheroma. *Eur Heart J*. 2008;29:1136-46.
28. Kobayashi N, Takano M, Tsurumi M, Shibata Y, Nishigoori S, Uchiyama S, Okazaki H, Shirakabe A, Seino Y, Hata N, Shimizu W. Features and outcomes of patients with calcified nodules at culprit lesions of acute coronary syndrome: an optical coherence tomography study. *Cardiology*. 2018;139:90-100.
29. Sugiyama T, Yamamoto E, Fracassi F, Lee H, Yonetsu T, Kakuta T, Soeda T, Saito Y, Yan BP, Kurihara O, Takano M, Niccoli G, Crea F, Higuma T, Kimura S, Minami Y, Ako J, Adriaenssens T, Boeder NF, Nef HM, Fujimoto JG, Fuster V, Finn AV, Falk E, Jang IK. Calcified plaques in patients with acute coronary syndromes. *JACC Cardiovasc Interv*. 2019;12:531-40.
30. Pasupathy S, Air T, Dreyer RP, Tavella R, Beltrame JF. Systematic review of patients presenting with suspected myocardial infarction and nonobstructive coronary arteries. *Circulation*. 2015;131:861-70.
31. Agewall S, Beltrame JF, Reynolds HR, Niessner A, Rosano G, Caforio AL, De Caterina R, Zimarino M, Roffi M, Kjeldsen K, Atar D, Kaski JC, Sechtem U, Tornvall P; WG on Cardiovascular Pharmacotherapy. ESC working group position paper on myocardial infarction with non-obstructive coronary arteries. *Eur Heart J*. 2017;38:143-53.
32. Reynolds HR, Srichai MB, Iqbal SN, Slater JN, Mancini GB, Feit F, Pena-Sing I, Axel L, Attubato MJ, Yatskar L, Kalhorn RT, Wood DA, Lobach IV, Hochman JS. Mechanisms of myocardial infarction in women without angiographically obstructive coronary artery disease. *Circulation*. 2011;124:1414-25.

33. Hong MK, Park SW, Lee CW, Ko JY, Kang DH, Song JK, Kim JJ, Mintz GS, Park SJ. Intravascular ultrasound findings of negative arterial remodeling at sites of focal coronary spasm in patients with vasospastic angina. *Am Heart J*. 2000;140:395-401.
34. Saito S, Yamagishi M, Takayama T, Chiku M, Koyama J, Ito K, Higashikata T, Seguchi O, Honye J, Kanmatsuse K. Plaque morphology at coronary sites with focal spasm in variant angina study using intravascular ultrasound. *Circ J*. 2003;67:1041-5.
35. Shin ES, Ann SH, Singh GB, Lim KH, Yoon HJ, Hur SH, Her AY, Koo BK, Akasaka T. OCT-defined morphological characteristics of coronary artery spasm sites in vasospastic angina. *JACC Cardiovasc Imaging*. 2015;8:1059-67.
36. Ghadri JR, Cammann VL, Jurisic S, Seifert B, Napp LC, Diekmann J, Bataiosu DR, D'Ascenzo F, Ding KJ, Sarcon A, Kazemian E, Birri T, Ruschitzka F, Luscher TF, Templin C. A novel clinical score (InterTAK Diagnostic Score) to differentiate takotsubo syndrome from acute coronary syndrome: results from the International Takotsubo Registry. *Eur J Heart Fail*. 2017;19:1036-42.
37. Eitel I, Stiermaier T, Graf T, Moller C, Rommel KP, Eitel C, Schuler G, Thiele H, Desch S. Optical coherence tomography to evaluate plaque burden and morphology in patients with takotsubo syndrome. *J Am Heart Assoc*. 2016;5:e004474.
38. Mortensen KH, Thuesen L, Kristensen IB, Christiansen EH. Spontaneous coronary artery dissection: a Western Denmark Heart Registry study. *Catheter Cardiovasc Interv*. 2009;74:710-7.
39. Vanzetto G, Berger-Coz E, Barone-Rochette G, Chavanon O, Bouvaist H, Hacin R, Blin D, Machecourt J. Prevalence, therapeutic management and medium-term prognosis of spontaneous coronary artery dissection: results from a database of 11,605 patients. *Eur J Cardiothorac Surg*. 2009;35:250-4.
40. Nishiguchi T, Tanaka A, Ozaki Y, Taruya A, Fukuda S, Taguchi H, Iwaguro T, Ueno S, Okumoto Y, Akasaka T. Prevalence of spontaneous coronary artery dissection in patients with acute coronary syndrome. *Eur Heart J Acute Cardiovasc Care*. 2016;5:263-70.
41. Saw J. Coronary angiogram classification of spontaneous coronary artery dissection. *Catheter Cardiovasc Interv*. 2014;84:1115-22.
42. Saw J, Mancini GB, Humphries K, Fung A, Boone R, Starovoytov A, Aymong E. Angiographic appearance of spontaneous coronary artery dissection with intramural hematoma proven on intracoronary imaging. *Catheter Cardiovasc Interv*. 2016;87:E54-E61.
43. Alfonso F, Canales E, Aleong G. Spontaneous coronary artery dissection: diagnosis by optical coherence tomography. *Eur Heart J*. 2009;30:385.
44. Jackson R, Al-Hussaini A, Joseph S, van Soest G, Wood A, Macaya F, Gonzalo N, Cade J, Caixeta A, Hlinomaz O, Leinveber P, O'Kane P, Garcia-Guimaraes M, Cortese B, Samani NJ, Escaned J, Alfonso F, Johnson T, Adlam D. Spontaneous coronary artery dissection: pathophysiological insights from optical coherence tomography. *JACC Cardiovasc Imaging*. 2019; doi: 10.1016/j.jcmg. 2019.01.015.
45. Johnson TW, Smith D, Strange JW, Bucciarelli-Ducci C, Lowe R, Baumbach A. Spontaneous multivessel coronary intramural hematoma: an insight with OCT. *JACC Cardiovasc Imaging*. 2012;5:1070-1.
46. Adlam D, Alfonso F, Maas A, Vrints C; Writing Committee. European Society of Cardiology, acute cardiovascular care association, SCAD study group: a position paper on spontaneous coronary artery dissection. *Eur Heart J*. 2018;39:3353-68.
47. Macaya F, Salazar CH, Pérez-Vizcayno MJ, Salinas P, Jiménez-Quevedo P, Nombela-Franco L, Del Trigo M, Núñez-Gil I, Fernández-Ortiz A, Macaya C, Escaned J, Gonzalo N. Feasibility and safety of intracoronary imaging for diagnosing spontaneous coronary artery dissection. *JACC Cardiovasc Imaging*. 2019;12:763-4.
48. Muller JE, Tofler GH, Stone PH. Circadian variation and triggers of onset of acute cardiovascular disease. *Circulation*. 1989;79:733-43.
49. Falk E. Plaque rupture with severe pre-existing stenosis precipitating coronary thrombosis. Characteristics of coronary atherosclerotic plaques underlying fatal occlusive thrombi. *Br Heart J*. 1983;50:127-34.
50. Constantinides P. Plaque fissures in human coronary thrombosis. *J Atheroscler Res*. 1966;6:1-17.
51. Burke AP, Farb A, Malcom GT, Liang YH, Smialek J, Virmani R. Coronary risk factors and plaque morphology in men with coronary disease who died suddenly. *N Engl J Med*. 1997;336:1276-82.
52. Virmani R, Kolodgie FD, Burke AP, Finn AV, Gold HK, Tulenko TN, Wrenn SP, Narula J. Atherosclerotic plaque progression and vulnerability to rupture: angiogenesis as a source of intraplaque hemorrhage. *Arterioscler Thromb Vasc Biol*. 2005;25:2054-61.
53. Pu J, Mintz GS, Biro S, Lee JB, Sum ST, Madden SP, Burke AP, Zhang P, He B, Goldstein JA, Stone GW, Muller JE, Virmani R, Maehara A. Insights into echoattenuated plaques, echolucent plaques, and plaques with spotty calcification: novel findings from comparisons among intravascular ultrasound, near-infrared spectroscopy, and pathological histology in 2,294 human coronary artery segments. *J Am Coll Cardiol*. 2014;63:2220-33.
54. Stone GW, Maehara A, Lansky AJ, de Bruyne B, Cristea E, Mintz GS, Mehran R, McPherson J, Farhat N, Marso SP, Parise H, Templin B, White R, Zhang Z, Serruys PW; PROSPECT Investigators. A prospective natural-history study of coronary atherosclerosis. *N Engl J Med*. 2011;364:226-35.
55. Calvert PA, Obaid DR, O'Sullivan M, Shapiro LM, McNab D, Densem CG, Schofield PM, Braganza D, Clarke SC, Ray KK, West NE, Bennett MR. Association between IVUS findings and adverse outcomes in patients with coronary artery disease: the VIVA (VH-IVUS in Vulnerable Atherosclerosis) Study. *JACC Cardiovasc Imaging*. 2011;4:894-901.
56. Garcia-Garcia HM, Mintz GS, Lerman A, Vince DG, Margolis MP, van Es GA, Morel MA, Nair A, Virmani R, Burke AP, Stone GW, Serruys PW. Tissue characterisation using intravascular radiofrequency data analysis: recommendations for acquisition, analysis, interpretation and reporting. *EuroIntervention*. 2009;5:177-89.
57. Mintz GS, Weisz G, Stone GW, Lee J-B, Pu J, Biro S, Maehara A, Abdel-Karim A-R, Brilakis ES, Banerjee S, Maini B. In vivo characterization of coronary plaques: novel findings from comparing greyscale and virtual histology intravascular ultrasound and near-infrared spectroscopy. *Eur Heart J*. 2011;33:372-83.
58. Gardner CM, Tan H, Hull EL, Lissauskas JB, Sum ST, Meese TM, Jiang C, Madden SP, Caplan JD, Burke AP, Virmani R, Goldstein J, Muller JE. Detection of lipid core coronary plaques in autopsy specimens with a novel catheter-based nearinfrared spectroscopy system. *JACC Cardiovasc Imaging*. 2008;1:638-48.
59. Goldstein JA, Maini B, Dixon SR, Brilakis ES, Grines CL, Rizik DG, Powers ER, Steinberg DH, Shunk KA, Weisz G, Moreno PR, Kini A, Sharma SK, Hendricks MJ, Sum ST, Madden SP, Muller JE, Stone GW, Kern MJ. Detection of lipid-core plaques by intracoronary near-infrared spectroscopy identifies high risk of periprocedural myocardial infarction. *Circ Cardiovasc Interv*. 2011;4:429-37.
60. Kang SJ, Mintz GS, Pu J, Sum ST, Madden SP, Burke AP, Xu K, Goldstein JA, Stone GW, Muller JE, Virmani R, Maehara A. Combined IVUS and NIRS detection of fibroatheromas: histopathological validation in human coronary arteries. *JACC Cardiovasc Imaging*. 2015;8:184-94.
61. Madder RD, Husaini M, Davis AT, VanOosterhout S, Khan M, Wohns D, McNamara RF, Wolschleger K, Gribar J, Collins JS, Jacoby M, Decker JM, Hendricks M, Sum ST, Madden S, Ware JH, Muller JE. Large lipid-rich coronary plaques detected by near-infrared spectroscopy at non-stented sites in the target artery identify patients likely to experience future major adverse cardiovascular events. *Eur Heart J Cardiovasc Imaging*. 2016;17:393-9.
62. Karlsson S, Anesäter E, Fransson K, Andell P, Persson J, Erlinge D. Intracoronary near-infrared spectroscopy and the risk of future cardiovascular events. *Open Heart*. 2019;6:e000917.

63. Oemrawsingh RM, Cheng JM, Garcia-Garcia HM, van Geuns RJ, de Boer SP, Simsek C, Kardys I, Lenzen MJ, van Domburg RT, Regar E, Serruys PW, Akkerhuis KM, Boersma E; ATHEROREMO-NIRS Investigators. Near-infrared spectroscopy predicts cardiovascular outcome in patients with coronary artery disease. *J Am Coll Cardiol*. 2014;64:2510-8.
64. Danek BA, Karatasakis A, Karacsonyi J, Alame A, Resendes E, Kalsaria P, Nguyen-Trong PJ, Rangan BV, Roesle M, Abdullah S, Banerjee S, Brilakis ES. Long-term follow-up after near-infrared spectroscopy coronary imaging: insights from the lipid cORE plaque association with CLinical events (ORACLE-NIRS) registry. *Cardiovasc Revasc Med*. 2017;18:177-81.
65. Waksman R, Torguson R, Spad MA, Garcia-Garcia H, Ware J, Wang R, Madden S, Shah P, Muller J. The Lipid-Rich Plaque Study of vulnerable plaques and vulnerable patients: study design and rationale. *Am Heart J*. 2017;192:98-104.
66. Waksman R. Assessment of coronary near-infrared spectroscopy imaging to detect vulnerable plaques and vulnerable patients. The Lipid-Rich Plaque study. *Transcatheter Cardiovascular Therapeutics* 2018; 21-25 September (San Diego, CA).
67. Xing L, Higuma T, Wang Z, Aguirre AD, Mizuno K, Takano M, Dauerman HL, Park SJ, Jang Y, Kim CJ, Kim SJ, Choi SY, Itoh T, Uemura S, Lowe H, Walters DL, Barlis P, Lee S, Lerman A, Toma C, Tan JWC, Yamamoto E, Bryniarski K, Dai J, Zanchin T, Zhang S, Yu B, Lee H, Fujimoto J, Fuster V, Jang IK. Clinical significance of lipid-rich plaque detected by optical coherence tomography: a 4-year follow-up study. *J Am Coll Cardiol*. 2017;69:2502-13.
68. Zheng B, Mintz GS, McPherson JA, De Bruyne B, Farhat NZ, Marso SP, Serruys PW, Stone GW, Maehara A. Predictors of plaque rupture within non-culprit fibroatheromas in patients with acute coronary syndromes: the PROSPECT study. *JACC Cardiovasc Imaging*. 2015;8:1180-7.
69. Stone PH, Saito S, Takahashi S, Makita Y, Nakamura S, Kawasaki T, Takahashi A, Katsuki T, Nakamura S, Namiki A, Hirohata A, Matsumura T, Yamazaki S, Yokoi H, Tanaka S, Otsuji S, Yoshimachi F, Honye J, Harwood D, Reitman M, Coskun AU, Papafaklis MI, Feldman CL; PREDICTION Investigators. Prediction of progression of coronary artery disease and clinical outcomes using vascular profiling of endothelial shear stress and arterial plaque characteristics: the PREDICTION Study. *Circulation*. 2012;126:172-81.
70. Cheng JM, Garcia-Garcia HM, de Boer SP, Kardys I, Heo JH, Akkerhuis KM, Oemrawsingh RM, van Domburg RT, Ligthart J, Witberg KT, Regar E, Serruys PW, van Geuns RJ, Boersma E. In vivo detection of high-risk coronary plaques by radiofrequency intravascular ultrasound and cardiovascular outcome: results of the ATHEROREMO-IVUS study. *Eur Heart J*. 2014;35:639-47.
71. Koskinas KC, Ughi GJ, Windecker S, Tearney GJ, Räber L. Intracoronary imaging of coronary atherosclerosis: validation for diagnosis, prognosis and treatment. *Eur Heart J*. 2016;37:524-35.
72. Bourantas CV, Garcia-Garcia HM, Torii R, Zhang YJ, Westwood M, Crake T, Serruys PW. Vulnerable plaque detection: an unrealistic quest or a feasible objective with a clinical value? *Heart*. 2016;102:581-9.
73. Hoogendoorn A, Gnanadesigan M, Zahnd G, van Ditzhuijzen NS, Schuurbiers JC, van Soest G, Regar E, Wentzel JJ. OCT-measured plaque free wall angle is indicative for plaque burden: overcoming the main limitation of OCT? *Int J Cardiovasc Imaging*. 2016;32:1477-81.
74. Inaba S, Mintz GS, Farhat NZ, Fajadet J, Dudek D, Marzocchi A, Templin B, Weisz G, Xu K, de Bruyne B, Serruys PW, Stone GW, Maehara A. Impact of positive and negative lesion site remodeling on clinical outcomes: insights from PROSPECT. *JACC Cardiovasc Imaging*. 2014;7:70-8.
75. Markis JE, Joffe CD, Cohn PF, Feen DJ, Herman MV, Gorlin R. Clinical significance of coronary arterial ectasia. *Am J Cardiol*. 1976;37:217-22.
76. Kruger D, Stierle U, Herrmann G, Simon R, Sheikhzadeh A. Exercise-induced myocardial ischemia in isolated coronary artery ectasias and aneurysms ("dilated coronopathy"). *J Am Coll Cardiol*. 1999;34:1461-70.
77. Hartnell GG, Parnell BM, Pridie RB. Coronary artery ectasia. Its prevalence and clinical significance in 4993 patients. *Br Heart J*. 1985;54:392-5.
78. Waterhouse BR, Tulloh RMR, Kim Y, Creasy W, Adlam D, Johnson TW. Retrospective study of the impact of unrecognised Kawasaki disease, coronary aneurysm and ectasia. *Int J Cardiol*. 2017;248:308-13.
79. Maehara A, Mintz GS, Ahmed JM, Fuchs S, Castagna MT, Pichard AD, Satler LF, Waksman R, Suddath WO, Kent KM, Weissman NJ. An intravascular ultrasound classification of angiographic coronary artery aneurysms. *Am J Cardiol*. 2001;88:365-70.
80. McCrindle BW, Rowley AH, Newburger JW, Burns JC, Bolger AF, Gewitz M, Baker AL, Jackson MA, Takahashi M, Shah PB, Kobayashi T, Wu M-H, Saji TT, Pahl E. Diagnosis, treatment, and long-term management of kawasaki disease: a scientific statement for health professionals from the American Heart Association. *Circulation*. 2017;135:e927-99.
81. Swaye PS, Fisher LD, Litwin P, Vignola PA, Judkins MP, Kemp HG, Mudd JG, Gosselin AJ. Aneurysmal coronary artery disease. *Circulation*. 1983;67:134-8.
82. Murthy PA, Mohammed TL, Read K, Gilkeson RC, White CS. MDCT of coronary artery aneurysms. *AJR Am J Roentgenol*. 2005;184:S19-20.
83. Gordon JB, Daniels LB, Kahn AM, Jimenez-Fernandez S, Vejar M, Numano F, Burns JC. The spectrum of cardiovascular lesions requiring intervention in adults after Kawasaki disease. *JACC Cardiovasc Interv*. 2016;9:687-96.
84. Mitomo S, Jabbour RJ, Watanabe Y, Mangieri A, Ancona M, Regazzoli D, Tanaka A, Nakajima A, Naganuma T, Giannini F, Latib A, Nakamura S, Colombo A. Comparison of mid-term clinical outcomes after treatment of ostial right coronary artery lesions with early and new generation drug-eluting stents: insights from an international multicenter registry. *Int J Cardiol*. 2018;254:53-8.
85. Mintz GS, Lefèvre T, Lassen JF, Testa L, Pan M, Singh J, Stankovic G, Banning AP. Intravascular ultrasound in the evaluation and treatment of left main coronary artery disease: a consensus statement from the European Bifurcation Club. *EuroIntervention*. 2018;14:e467-74.
86. Pérez-Pomares JM, de la Pompa JL, Franco D, Henderson D, Ho SY, Houyel L, Kelly RG, Sedmera D, Sheppard M, Sperling S, Thiene G, van den Hoff M, Basso C. Congenital coronary artery anomalies: a bridge from embryology to anatomy and pathophysiology—a position statement of the development, anatomy, and pathology ESC Working Group. *Cardiovasc Res*. 2016;109:204-16.
87. Kim SY, Seo JB, Do KH, Heo JN, Lee JS, Song JW, Choe YH, Kim TH, Yong HS, Choi SI, Song KS, Lim TH. Coronary artery anomalies: classification and ECG-gated multi-detector row CT findings with angiographic correlation. *Radiographics*. 2006;26:317-33; discussion 333-4.
88. Fabris E, Kilic ID, Caiazzo G, Serdoz R, Foin N, Sinagra G, Di Mario C. Nonatherosclerotic coronary artery narrowing. *JACC Cardiovasc Imaging*. 2016;9:317-20.
89. Galie N, Saia F, Palazzini M, Manes A, Russo V, Bacchi Reggiani ML, Dall'Ara G, Monti E, Dardi F, Albini A, Rinaldi A, Gotti E, Taglieri N, Marrozzini C, Lovato L, Zompatori M, Marzocchi A. Left main coronary artery compression in patients with pulmonary arterial hypertension and angina. *J Am Coll Cardiol*. 2017;69:2808-17.
90. Ruisi M, Fallahi A, Lala M, Kanei Y. Aortic dissection presenting as acute subtotal left main coronary artery occlusion: a case approach and review of the literature. *J Clin Med Res*. 2015;7:356-60.
91. Ueki Y, Kadner A, Gräni C, Räber L. ST-segment elevation myocardial infarction due to optical coherence tomography-detected coronary artery compression following supra-avalvular pulmonary artery patchplasty 18 years after switch procedure. *JACC Cardiovasc Interv*. 2018;11:e149-51.
92. Chih S, Chong AY, Mielniczuk LM, Bhatt DL, Beanlands RS. Allograft vasculopathy: the Achilles' heel of heart transplantation. *J Am Coll Cardiol*. 2016;68:80-91.

93. Kobashigawa JA, Tobis JM, Starling RC, Tuzcu EM, Smith AL, Valentine HA, Yeung AC, Mehra MR, Anzai H, Oeser BT, Abeywickrama KH, Murphy J, Cretin N. Multicenter intravascular ultrasound validation study among heart transplant recipients. *J Am Coll Cardiol.* 2005;45:1532.
94. Hernandez JM, de Prada JA, Burgos V, Sainz Laso F, Valls MF, Vilchez FG, Llano M, Ruano J, Zueco J, Colman T, Duran RM. Virtual histology intravascular ultrasound assessment of cardiac allograft vasculopathy from 1 to 20 years after heart transplantation. *J Heart Lung Transplant.* 2009;28:156-62.
95. Okada K, Fearon WF, Luikart H, Kitahara H, Otagiri K, Tanaka S, Kimura T, Yock PG, Fitzgerald PJ, Yeung AC, Valentine HA, Khush KK, Honda Y. Attenuated-signal plaque progression predicts long-term mortality after heart transplantation: IVUS assessment of cardiac allograft vasculopathy. *J Am Coll Cardiol.* 2016;68:382-92.
96. Cassar A, Matsuo Y, Herrmann J, Li J, Lennon RJ, Gulati R, Lerman LO, Kushwaha SS, Lerman A. Coronary atherosclerosis with vulnerable plaque and complicated lesions in transplant recipients: new insight into cardiac allograft vasculopathy by optical coherence tomography. *Eur Heart J.* 2013;34:2610-7.
97. Ichibori Y, Ohtani T, Nakatani D, Tachibana K, Yamaguchi O, Toda K, Akasaka T, Fukushima N, Sawa Y, Komuro I, Kotani J, Sakata Y. Optical coherence tomography and intravascular ultrasound evaluation of cardiac allograft vasculopathy with and without intimal neovascularization. *Eur Heart J Cardiovasc Imaging.* 2016;17:51-8.
98. Badano LP, Miglioranza MH, Edvardsen T, Colafranceschi AS, Muraru D, Bacal F, Nieman K, Zoppellaro G, Marcondes Braga FG, Binder T, Habib G, Lancellotti P, Sicari R, Cosyns B, Donal E, Lombardi M, Sarvari S; Document reviewers. European Association of Cardiovascular Imaging/Cardiovascular Imaging Department of the Brazilian Society of Cardiology recommendations for the use of cardiac imaging to assess and follow patients after heart transplantation. *Eur Heart J Cardiovasc Imaging.* 2015;16:919-48.
99. Bech GJ, De Bruyne B, Pijls NH, de Muinck ED, Hoorntje JC, Escaned J, Stella PR, Boersma E, Bartunek J, Koolen JJ, Wijns W. Fractional flow reserve to determine the appropriateness of angioplasty in moderate coronary stenosis: a randomized trial. *Circulation.* 2001;103:2928-34.
100. De Bruyne B, Pijls NH, Kalesan B, Barbato E, Tonino PA, Piroth Z, Jagic N, Mobius-Winkler S, Rioufol G, Witt N, Kala P, MacCarthy P, Engstrom T, Oldroyd KG, Mavromatis K, Manoharan G, Verlee P, Frobert O, Curzen N, Johnson JB, Juni P, Fearon WF; FAME 2 Trial Investigators. Fractional flow reserve-guided PCI versus medical therapy in stable coronary disease. *N Engl J Med.* 2012;367:991-1001.
101. Tonino PA, De Bruyne B, Pijls NH, Siebert U, Ikeno F, van't Veer M, Klauss V, Manoharan G, Engstrom T, Oldroyd KG, Ver Lee PN, MacCarthy PA, Fearon WF; FAME Study Investigators. Fractional flow reserve versus angiography for guiding percutaneous coronary intervention. *N Engl J Med.* 2009;360:213-24.
102. Davies JE, Sen S, Dehbi HM, Al-Lamee R, Petraco R, Nijjer SS, Bhandi R, Lehman SJ, Walters D, Sapontis J, Janssens L, Vrints CJ, Khashaba A, Laine M, Van Belle E, Krackhardt F, Bojara W, Going O, Harle T, Indolfi C, Niccoli G, Ribichini F, Tanaka N, Yokoi H, Takashima H, Kikuta Y, Erglis A, Vinhas H, Canas Silva P, Baptista SB, Alghamdi A, Hellig F, Koo BK, Nam CW, Shin ES, Doh JH, Brugaletta S, Alegria-Barrero E, Meuwissen M, Piek JJ, van Royen N, Sezer M, Di Mario C, Gerber RT, Malik IS, Sharp ASP, Talwar S, Tang K, Samady H, Altman J, Seto AH, Singh J, Jeremias A, Matsuo H, Kharbanda RK, Patel MR, Serruys P, Escaned J. Use of the instantaneous wave-free ratio or fractional flow reserve in PCI. *N Engl J Med.* 2017;376:1824-34.
103. Gotberg M, Christiansen EH, Gudmundsdottir IJ, Sandhall L, Danielewicz M, Jakobsen L, Olsson SE, Ohagen P, Olsson H, Omerovic E, Calais F, Lindroos P, Maeng M, Todt T, Venetsanos D, James SK, Karegren A, Nilsson M, Carlsson J, Hauer D, Jensen J, Karlsson AC, Panayi G, Erlinge D, Frobert O; iFRSWEDEHEART Investigators. Instantaneous wave-free ratio versus fractional flow reserve to guide PCI. *N Engl J Med.* 2017;376:1813-23.
104. Lindstaedt M, Spiecker M, Perings C, Lawo T, Yazar A, Holland-Letz T, Muegge A, Bojara W, Germing A. How good are experienced interventional cardiologists at predicting the functional significance of intermediate or equivocal left main coronary artery stenoses? *Int J Cardiol.* 2007;120:254-61.
105. de la Torre Hernández JM, Hernández F, Alfonso F. The optimal cutoff value for left main minimal lumen area of 4.5 mm²: a word of caution. *JACC Cardiovasc Interv.* 2015;8:122-3.
106. Park SJ, Ahn JM, Kang SJ, Yoon SH, Koo BK, Lee JY, Kim WJ, Park DW, Lee SW, Kim YH, Lee CW, Park SW. Intravascular ultrasound-derived minimal lumen area criteria for functionally significant left main coronary artery stenosis. *JACC Cardiovasc Interv.* 2014;7:868-74.
107. Jasti V, Ivan E, Yalamanchili V, Wongpraparut N, Leesar MA. Correlations between fractional flow reserve and intravascular ultrasound in patients with an ambiguous left main coronary artery stenosis. *Circulation.* 2004;110:2831-6.
108. Rusinova RP, Mintz GS, Choi SY, Araki H, Hakim D, Sanidas E, Yakushiji T, Weisz G, Mehran R, Franklin-Bond T, Fahy M, Leon MB, Stone GW, Moses JW, Tahk SJ, Ochiai M, Maehara A. Intravascular ultrasound comparison of left main coronary artery disease between white and Asian patients. *Am J Cardiol.* 2013;111:979-84.
109. de la Torre Hernandez JM, Hernandez Hernandez F, Alfonso F, Rumoroso JR, Lopez-Palop R, Sadaba M, Carrillo P, Rondan J, Lozano I, Ruiz Nodar JM, Baz JA, Fernandez Nofrerias E, Pajin F, Garcia Camarero T, Gutierrez H; LITRO Study Group (Spanish Working Group on Interventional Cardiology). Prospective application of pre-defined intravascular ultrasound criteria for assessment of intermediate left main coronary artery lesions results from the multicenter LITRO study. *J Am Coll Cardiol.* 2011;58:351-8.
110. D'Ascenzo F, Barbero U, Cerrato E, Lipinski MJ, Omedè P, Montefusco A, Taha S, Naganuma T, Reith S, Voros S, Latib A, Gonzalo N, Quadri G, Colombo A, Biondi-Zoccai G, Escaned J, Moretti C, Gaita F. Accuracy of intravascular ultrasound and optical coherence tomography in identifying functionally significant coronary stenosis according to vessel diameter: a meta-analysis of 2,581 patients and 2,807 lesions. *Am Heart J.* 2015;169:663-73.
111. Gonzalo N, Escaned J, Alfonso F, Nolte C, Rodriguez V, Jimenez-Quevedo P, Banuelos C, Fernandez-Ortiz A, Garcia E, Hernandez-Antolin R, Macaya C. Morphometric assessment of coronary stenosis relevance with optical coherence tomography: a comparison with fractional flow reserve and intravascular ultrasound. *J Am Coll Cardiol.* 2012;59:1080-9.
112. Usui E, Yonetsu T, Kanaji Y, Hoshino M, Yamaguchi M, Hada M, Hamaya R, Kanno Y, Murai T, Lee T, Kakuta T. Efficacy of optical coherence tomography derived morphometric assessment in predicting the physiological significance of coronary stenosis: head-to-head comparison with intravascular ultrasound. *EuroIntervention.* 2018;13:e2210-8.
113. Koskinas KC, Nakamura M, Räber L, Colleran R, Kadota K, Capodanno D, Wijns W, Akasaka T, Valgimigli M, Guagliumi G, Windecker S, Byrne RA. Current use of intracoronary imaging in interventional practice—results of a European Association of Percutaneous Cardiovascular Interventions (EAPCI) and Japanese Association of Cardiovascular Interventions and Therapeutics (CVIT) Clinical Practice Survey. *EuroIntervention.* 2018;14:e475-84.

Supplementary data

Supplementary Table 1. Landmark studies examining the efficacy of intravascular imaging in assessing plaque characteristics using histology as gold standard.

Supplementary Table 2. Histology-based studies that examined the efficacy of CTCA in assessing plaque characteristics.

The supplementary data are published online at:
https://eurointervention.pconline.com/doi/10.4244/EIJY19M06_02



Supplementary Table 1. Landmark studies examining the efficacy of intravascular imaging in assessing plaque characteristics using histology as gold standard.

Plaque feature	Modality	Study	Sample size	Results
Lumen, vessel wall and plaque area	Grayscale IVUS (25MHz)	Potkin et al ¹	32 segments from 21 human coronary arteries; 54 cross sections	High correlations were noted between histology and IVUS estimations for the: <ul style="list-style-type: none"> • Lumen area (r=0.85, P<0.001) • Vessel wall area (r=0.94, P<0.001) • Plaque burden (r=0.84, P<0.001) and • Plaque thickness (r=0.92, P<0.001)
	OCT and grayscale IVUS (40MHz)	Kume et al. ²	54 segments from 54 human coronary arteries (18 human cadavers)	<ul style="list-style-type: none"> • There was a high correlation between the estimations of IVUS and OCT with the estimations of histology for the lumen area (r=0.96, P<0.001 and r=0.97, P<0.001 respectively) • A higher correlation was noted between OCT and histology than IVUS and histology for the intima media thickness (r=0.95, P<0.001 and r=0.88, P<0.001) • OCT but not IVUS was able to assess intima thickness; there was a good agreement between OCT and histology for the intima thickness (r=0.98, P<0.001)

**Plaque
composition**

Grayscale IVUS (25MHz)	Potkin et al. ¹	28 segments from 12 human coronary arteries; 28 cross sections	<ul style="list-style-type: none"> The analyzed frames were split in quadrants and tissue composition was estimated in each quadrant. IVUS was able to correctly identify all the calcific tissues (100%), 96% of the fibrotic and 78% of the lipid tissues
VH-IVUS	Nair et al. ³	88 cross sections selected from 51 left anterior descending coronary arteries; in these cross sections 277 regions of interest were defined, 208 were used for training and 56 for validation purposes	<ul style="list-style-type: none"> An excellent accuracy was noted between VH-IVUS and histology for fibrous (79.7%), fibrolipidic (81.2%), calcific (92.8%), and calcified-necrotic tissues (85.5%)
VH-IVUS	Thim et al. ⁴	18 cross sections from 18 lesions identified in 9 atherosclerotic pigs	<ul style="list-style-type: none"> VH-IVUS falsely detected a necrotic core in 5 out of the 6 lesions that did not have a necrotic core on histology There was no correlation between the necrotic core area estimated by VH-IVUS and the necrotic core area detected by histology
IB-IVUS	Kawasaki et al ⁵	88 regions selected from 18 human coronary arteries from 9 autopsied patients	<ul style="list-style-type: none"> IB-IVUS was able to identify lipid, fibrotic, calcific tissues and intima hyperplasia with high accuracy

OCT	Yabushita et al. ⁶	357 diseased human arterial segments obtained from the aorta (n=162), carotids (n=105) and coronary arteries (n=90) from 90 human cadavers; 50 segments were used for training and 307 for validation purposes	<ul style="list-style-type: none"> • Plaque characterisation in OCT was performed by two experts. • Both experts were able to detect plaque composition using OCT with a high sensitivity and specificity: fibrotic (range: 71-79% and 97-98% respectively), fibrocalcific (range: 95-96% and 97-97% respectively) and lipidic tissues (range: 90-94% and 90-92% respectively)
OCT	Manfrini et al. ⁷	68 cross sections obtained from 15 necropsy cases	<ul style="list-style-type: none"> • OCT was able to correctly identify 45% of the fibroatheromas, 68% of the fibrocalcific plaques, 83% of the fibrotic plaques and 100% of the complicated lesions • OCT misinterpretation was caused mainly by the limited tissue penetration of the OCT signal and the limited efficacy of the modality to distinguish lipid from calcific tissue
NIRS	Gardner et al. ⁸	126 coronary segments from 51 human hearts; analysis was performed at 2mm intervals – 2,496 blocks were included in the analysis	<ul style="list-style-type: none"> • The block chemogram was able to accurately detect lipid cores (defined as a lipid core >60° in circumferential extent, >200µm thick, with a mean fibrous cap thickness <450µm) with an AUC of 0.80
OCT	Tearney et al. ⁹	26 lipid rich plaques (19 aortas and 7 carotid bulbs) obtained from 17 randomly selected	<ul style="list-style-type: none"> • Analysis was performed only in the fibrous cap located over the centre of lipid-rich plaques.

Macrophages	OCT	Phipps et al ¹⁰	1599 cross sections obtained from 14 human coronary arteries from 10 human hearts cadavers	<ul style="list-style-type: none"> • A significant association was reported between the normalised standard deviation of the OCT signal and macrophages' density in the fibrous cap (r=0.84, P<0.001) • Macrophages were present in 57% of the bright spot positive regions • Other causes of bright-spots on OCT were fibrous tissue (8%), interfaces between calcium and fibrous tissue (10%), calcium and lipid (5%) and fibrous cap and lipid pool (3%) • Macrophage accumulations were also detected in dark regions in OCT images
Neovessels	OCT	Kume et al ¹¹	55 plaques from 31 human cadavers	<ul style="list-style-type: none"> • OCT had a low sensitivity 52% and moderate specificity 68% in detecting neovessels
Fibrous cap thickness	OCT	Kume et al. ¹²	35 lipid-rich plaques identified in 102 coronary arteries obtained from 38 human cadavers	<ul style="list-style-type: none"> • There was a high agreement between histology and OCT estimations for the fibrous cap thickness (r=0.90, P<0.001, mean difference: -24±44µm) • The intra and inter-observer variability between observers estimations were 13±41µm and 20±59µm respectively
Thrombus	OCT	Kume et al. ¹³	108 coronary artery segments from 40 human cadavers	<ul style="list-style-type: none"> • Red thrombi appeared in OCT as high-backscattering protrusions in the lumen with a signal free shadowing behind, while white thrombi appeared

as low-backscattering protrusions with no shadowing

- The distance peak to 50% drop in signal intensity was able to differentiate red from white thrombus with a high sensitivity and specificity (90% and 88% respectively)

Table footnote: AUC, area under the curve; IB, integrated backscatter; IVUS, intravascular ultrasound; NIRS, near infrared spectroscopy; OCT, optical coherence tomography; VH, virtual histology.

Supplementary Table 2. Histology-based studies that examined the efficacy of CTCA in assessing plaque characteristics.

Study	Objective	Imaging modality	Sample size	Results
Becker et al. ¹⁴	To evaluate the efficacy of CTCA in assessing plaque composition	4-slice CTCA	50 lesions detected in the coronary arteries of 11 autopsy cases	<ul style="list-style-type: none"> CTCA had a moderate sensitivity for detecting atheroma (73%) and fibroatheroma (70%) and an excellent sensitivity for detecting fibrocalcific (86%) and calcific plaques (100%)
Knollmann et al. ¹⁴	To evaluate the efficacy of CTCA in assessing the size of different plaque components	16-slice CTCA	226 segments from 30 autopsy hearts	<ul style="list-style-type: none"> A high correlation was noted between the log-transformed plaque areas and the calcific areas estimated by CTCA and histology ($r=0.73$, $P<0.0001$ and $r=0.83$, $P<0.0001$ respectively); the correlation however was weaker between the estimations of CTCA and histology for the non-calcific and lipid areas ($r=0.53$, $P<0.0001$ and $r=0.43$, $P<0.0001$ respectively)
Leschka et al. ¹⁵	To investigate the ability of dual-source CTCA in characterising plaque composition	2x64-slice CTCA imaging	322 plaques identified in the coronary arteries of 25 cadaveric hearts	<ul style="list-style-type: none"> CTCA was able to detect 79% of the plaques identified by histology CTCA had high sensitivity and specificity for detecting calcified plaques (80% and 95% respectively) Non-calcified plaques in CTCA corresponded with an excellent sensitivity (100%) and

moderate specificity (72%) to early atherosclerotic plaques

- Mixed/calcified plaques in CTCA corresponded with a high sensitivity (92%, 89%) and excellent specificity (100%) to advanced plaques

Chopard et al. ¹⁶	To compare the performance of CTCA and IVUS in assessing plaque burden and composition	40MHz grayscale IVUS and 64-slice CTCA	83 cross sections detected in 21 RCA obtained from cadaveric hearts	<ul style="list-style-type: none">• IVUS enabled more accurate evaluation of minimum plaque thickness than CTCA ($r^2=0.70$ vs $r^2=0.49$)• IVUS and CTCA had a high sensitivity (100% vs 95%) and specificity (88% vs 100%) for detecting calcific plaques, CTCA was more accurate in detecting fibrotic plaque (sensitivity: 73% vs 66%; specificity: 85% vs 78%) while IVUS was more effective in detecting lipid-rich plaque (sensitivity: 70% vs 55%; specificity: IVUS 85% vs 90%)
Maurovich-Horvat et al. ¹⁷	To examine the efficacy of CTCA, IVUS and OCT in differentiating early from advanced atherosclerotic plaques	40 MHz grayscale IVUS, optical frequency domain imaging and 64-slice CTCA	379 cross sections from 9 arteries of 3 donor hearts; 293 sections were assessed by IVUS and 285 by OCT	<ul style="list-style-type: none">• OCT had a higher diagnostic accuracy than IVUS or CTCA in differentiating early from advanced atherosclerotic plaques (AUC: 0.858 vs 0.631 vs 0.697, $P<0.001$)

Maurovich-Horvat et al. ¹⁸	To investigate whether plaque patterns in CTCA can identify advanced atherosclerotic plaques in histology	64-slice CTCA	611 cross sections from 21 coronary arteries of 7 donor hearts	<ul style="list-style-type: none"> • Homogenous and heterogeneous plaques in CTCA had moderate specificity (62.6% and 67.3%, respectively) while a napkin ring sign in CTCA had an excellent specificity in detecting advanced lesions (98.9%) • The diagnostic accuracy of the pattern-based scheme to identify advanced plaques was superior to the accuracy of the conventional plaque characterisation scheme (AUC: 0.761 vs. 0.678, P<0.001).
Schlett et al. ¹⁹	To evaluate the efficacy of CTCA in detecting LCP identified by histology or OCT imaging	Time domain-OCT and 64-slice CTCA	446 histological cross sections obtained from the coronary arteries of 5 donor hearts	<ul style="list-style-type: none"> • Low attenuated area in CTCA (cutoff of <60HU) was associated with the lipid area in histology (r=0.53, P<0.0001) • An attenuated plaque (<60HU) with an absolute area >1mm² or a relative area >25% was able to detect LCP in histology with an AUC of 0.744 and 0.722 respectively • An attenuated plaque (<60HU) with an absolute area >1mm² or a relative area >25% was able to detect LCP in OCT with an AUC of 0.644 and 0.751 respectively
Schlett et al. ²⁰	To assess the effect of plaque segmentation on the accuracy of CTCA in detecting LCP	40MHz grayscale IVUS and 64-slice CTCA	446 cross-sections from the coronary arteries of 5 donor hearts	<ul style="list-style-type: none"> • Two methodologies for the delineation of the plaque area were tested: in the first the plaque area was defined as the area between the lumen and the outer vessel wall border while in the second the non-calcified plaque was traced directly • The HU values in the second method enabled more accurate identification of LCP than

Obaid et al. ²¹	To assess the efficacy of CTCA in assess plaque morphology	IVUS-VH and 64-slice dual source CTCA	87 segments from 8 LAD obtained from 8 donor hearts; 72 segments were studied by IVUS-VH	<p>the HU values in the first method (AUC: 0.831 vs 0.780, P=0.005)</p> <ul style="list-style-type: none"> • IVUS-VH had a higher diagnostic accuracy than CTCA in detecting atherosclerotic plaques (99% vs 91%) • CTCA had a marginally superior accuracy comparing to IVUS-VH in identifying calcified plaques (82% vs 75%) and calcified fibroatheromas (80% vs 75%) and similar accuracy for detecting fibroatheromas (80% vs 79%) • CTCA was unable to identify TCFA while the diagnostic accuracy of IVUS-VH for TCFA was 82%
Obaid et al. ²²	To compare the accuracy of DECT and SECT in detecting plaque components	64-slice dual source CTCA	77 segments from 7 LAD obtained from 7 cadaveric hearts	<ul style="list-style-type: none"> • SECT and a cut-off of <93HU was able to detect necrotic core with a moderate sensitivity, specificity and accuracy (50%, 94% and 78% respectively) • DECT metrics had a superior efficacy in detecting necrotic core (sensitivity: 64% specificity: 98% and accuracy 86%) than SECT
Puncher et al. ²³	To examine whether iterative reconstruction algorithms improve the efficacy of CTCA	64-slice CTCA – 3 methodologies were used to reconstructed	173 cross sections from 3 ex vivo human donor hearts	<ul style="list-style-type: none"> • A <60HU cut-off on CTCA images enabled detection of LCP in all the 3 reconstruction techniques. • MBIR had the highest diagnostic accuracy in detecting LCP than FBP or ASIR

in detecting LCP

the raw data FBP,

(0.903 vs 0.850 vs 0.803)

ASIR and MBIR

Han et al.²⁴

To assess the efficacy of a semi-automated CTCA segmentation method in detecting atheroma burden and composition

64-slice CTCA

105 cross-sections from 8 cadaveric hearts

- A significant correlation was reported between CTCA and histology for the vessel, lumen, plaque and calcific plaque areas ($r=0.69$, $r=0.72$, $r=0.51$ and 0.50 respectively; $P<0.001$ for all estimations).
- There was a weak correlation between CTCA and histology for the lipid area ($r=0.29$, $P=0.003$)
- A low attenuation ($<75\text{HU}$) plaque area $>0.14\text{mm}^2$ was able to detect with moderate accuracy lipid rich plaques (AUC: 0.65).

Table footnote: ASIR, adaptive statistical iterative reconstruction; AUC, area under the curve; CTCA, computed tomography coronary angiography; DECT, dual energy CT; FBR: filter back projection; IVUS, intravascular ultrasound; LAD, left anterior descending coronary artery; LCP, lipid core plaque; MBIR model-based iterative reconstruction; OCT, optical coherence tomography; RCA, right coronary artery; SECT, single energy CT; DECT, dual energy CT; TCFA, thin cap fibroatheroma; VH, virtual histology.

REFERENCES

1. Potkin BN, Bartorelli AL, Gessert JM, Neville RF, Almagor Y, Roberts WC, Leon MB. Coronary artery imaging with intravascular high-frequency ultrasound. *Circulation* 1990;81(5):1575-85.
2. Kume T, Akasaka T, Kawamoto T, Watanabe N, Toyota E, Neishi Y, Sukmawan R, Sadahira Y, Yoshida K. Assessment of coronary intima-media thickness by optical coherence tomography: comparison with intravascular ultrasound. *Circ J* 2005;69(8):903-7.
3. Nair A, Kuban BD, Tuzcu EM, Schoenhagen P, Nissen SE, Vince DG. Coronary plaque classification with intravascular ultrasound radiofrequency data analysis. *Circulation* 2002;106(17):2200-6.
4. Thim T, Hagensen MK, Wallace-Bradley D, Granada JF, Kaluza GL, Drouet L, Paaske WP, Botker HE, Falk E. Unreliable assessment of necrotic core by virtual histology intravascular ultrasound in porcine coronary artery disease. *Circ Cardiovasc Imaging* 2010;3(4):384-91.
5. Kawasaki M, Takatsu H, Noda T, Sano K, Ito Y, Hayakawa K, Tsuchiya K, Arai M, Nishigaki K, Takemura G, Minatoguchi S, Fujiwara T, Fujiwara H. In vivo quantitative tissue characterization of human coronary arterial plaques by use of integrated backscatter intravascular ultrasound and comparison with angioscopic findings. *Circulation* 2002;105(21):2487-92.
6. Yabushita H, Bouma BE, Houser SL, Aretz HT, Jang IK, Schlendorf KH, Kauffman CR, Shishkov M, Kang DH, Halpern EF, Tearney GJ. Characterization of human atherosclerosis by optical coherence tomography. *Circulation* 2002;106(13):1640-5.
7. Manfrini O, Mont E, Leone O, Arbustini E, Eusebi V, Virmani R, Bugiardini R. Sources of error and interpretation of plaque morphology by optical coherence tomography. *Am J Cardiol* 2006;98(2):156-9.
8. Gardner CM, Tan H, Hull EL, Lissauskas JB, Sum ST, Meese TM, Jiang C, Madden SP, Caplan JD, Burke AP, Virmani R, Goldstein J, Muller JE. Detection of lipid core coronary plaques in autopsy specimens with a novel catheter-based near-infrared spectroscopy system. *JACC Cardiovascular imaging* 2008;1(5):638-48.
9. Tearney GJ, Yabushita H, Houser SL, Aretz HT, Jang IK, Schlendorf KH, Kauffman CR, Shishkov M, Halpern EF, Bouma BE. Quantification of macrophage content in atherosclerotic plaques by optical coherence tomography. *Circulation* 2003;107(1):113-9.
10. Phipps JE, Vela D, Hoyt T, Halaney DL, Mancuso JJ, Buja LM, Asmis R, Milner TE, Feldman MD. Macrophages and intravascular OCT bright spots: a quantitative study. *JACC Cardiovascular imaging* 2015;8(1):63-72.
11. Kume T, Okura H, Yamada R, Koyama T, Fukuhara K, Kawamura A, Imai K, Neishi Y, Uemura S. Detection of Plaque Neovascularization by Optical Coherence Tomography: Ex Vivo Feasibility Study and In Vivo Observation in Patients With Angina Pectoris. *The Journal of invasive cardiology* 2016;28(1):17-22.
12. Kume T, Akasaka T, Kawamoto T, Okura H, Watanabe N, Toyota E, Neishi Y, Sukmawan R, Sadahira Y, Yoshida K. Measurement of the thickness of the fibrous cap by optical coherence tomography. *Am Heart J* 2006;152(4):755.e1-4.
13. Kume T, Akasaka T, Kawamoto T, Ogasawara Y, Watanabe N, Toyota E, Neishi Y, Sukmawan R, Sadahira Y, Yoshida K. Assessment of coronary arterial thrombus by optical coherence tomography. *Am J Cardiol* 2006;97(12):1713-7.
14. Knollmann F, Ducke F, Krist L, Kertesz T, Meyer R, Guski H, Felix R. Quantification of atherosclerotic coronary plaque components by submillimeter computed tomography. *Int J Cardiovasc Imaging* 2008;24(3):301-10.

15. Leschka S, Seitun S, Dettmer M, Baumuller S, Stolzmann P, Goetti R, Scheffel H, Feuchtner G, Wunnicke K, Wildermuth S, Oehlschlegel C, Marincek B, Jochum W, Alkadhi H. Ex vivo evaluation of coronary atherosclerotic plaques: characterization with dual-source CT in comparison with histopathology. *J Cardiovasc Comput Tomogr* 2010;4(5):301-8.
16. Chopard R, Boussel L, Motreff P, Rioufol G, Tabib A, Douek P, Meyronet D, Revel D, Finet G. How reliable are 40 MHz IVUS and 64-slice MDCT in characterizing coronary plaque composition? An ex vivo study with histopathological comparison. *Int J Cardiovasc Imaging* 2010;26(4):373-83.
17. Maurovich-Horvat P, Schlett CL, Alkadhi H, Nakano M, Stolzmann P, Vorpahl M, Scheffel H, Tanaka A, Warger WC, 2nd, Maehara A, Ma S, Kriegel MF, Kaple RK, Seifarth H, Bamberg F, Mintz GS, Tearney GJ, Virmani R, Hoffmann U. Differentiation of early from advanced coronary atherosclerotic lesions: systematic comparison of CT, intravascular US, and optical frequency domain imaging with histopathologic examination in ex vivo human hearts. *Radiology* 2012;265(2):393-401.
18. Maurovich-Horvat P, Schlett CL, Alkadhi H, Nakano M, Otsuka F, Stolzmann P, Scheffel H, Ferencik M, Kriegel MF, Seifarth H, Virmani R, Hoffmann U. The napkin-ring sign indicates advanced atherosclerotic lesions in coronary CT angiography. *JACC Cardiovasc Imaging* 2012;5(12):1243-52.
19. Schlett CL, Maurovich-Horvat P, Ferencik M, Alkadhi H, Stolzmann P, Scheffel H, Seifarth H, Nakano M, Do S, Vorpahl M, Kauczor HU, Bamberg F, Tearney GJ, Virmani R, Hoffmann U. Histogram analysis of lipid-core plaques in coronary computed tomographic angiography: ex vivo validation against histology. *Invest Radiol* 2013;48(9):646-53.
20. Schlett CL, Ferencik M, Celeng C, Maurovich-Horvat P, Scheffel H, Stolzmann P, Do S, Kauczor HU, Alkadhi H, Bamberg F, Hoffmann U. How to assess non-calcified plaque in CT angiography: delineation methods affect diagnostic accuracy of low-attenuation plaque by CT for lipid-core plaque in histology. *Eur Heart J Cardiovasc Imaging* 2013;14(11):1099-105.
21. Obaid DR, Calvert PA, Gopalan D, Parker RA, Hoole SP, West NE, Goddard M, Rudd JH, Bennett MR. Atherosclerotic plaque composition and classification identified by coronary computed tomography: assessment of computed tomography-generated plaque maps compared with virtual histology intravascular ultrasound and histology. *Circ Cardiovasc Imaging* 2013;6(5):655-64.
22. Obaid DR, Calvert PA, Gopalan D, Parker RA, West NE, Goddard M, Rudd JH, Bennett MR. Dual-energy computed tomography imaging to determine atherosclerotic plaque composition: a prospective study with tissue validation. *J Cardiovasc Comput Tomogr* 2014;8(3):230-7.
23. Puchner SB, Ferencik M, Maurovich-Horvat P, Nakano M, Otsuka F, Kauczor HU, Virmani R, Hoffmann U, Schlett CL. Iterative image reconstruction algorithms in coronary CT angiography improve the detection of lipid-core plaque--a comparison with histology. *Eur Radiol* 2015;25(1):15-23.
24. Han D, Torii S, Yahagi K, Lin FY, Lee JH, Rizvi A, Gransar H, Park MW, Roudsari HM, Stuijzand WJ, Baskaran L, B OH, Park HB, Lee SE, Ali Z, Kutys R, Chang HJ, Earls JP, Fowler D, Virmani R, Min JK. Quantitative measurement of lipid rich plaque by coronary computed tomography angiography: A correlation of histology in sudden cardiac death. *Atherosclerosis* 2018.